Exacerbation of diabetic nephropathy by hyperlipidaemia is mediated by toll-like receptor 4 in mice

T. Kuwabara, K. Mori, M. Mukoyama, M. Kasahara, H. Yokoi, Y. Saito, Y. Ogawa, H. Imamaki, T. Kawanishi, A. Ishii, K. Koga, K. P. Mori, Y. Kato, A. Sugawara, K. Nakao

T. Kuwabara, K. Mori*, M. Mukoyama, M. Kasahara, H. Yokoi, Y. Saito, H. Imamaki, T. Kawanishi, A. Ishii, K. Koga, K. P. Mori, Y. Kato, K. Nakao

Department of Medicine and Clinical Science, Kyoto University Graduate School of Medicine, 54 Shogoin Kawaharacho, Sakyoku, Kyoto 606-8507, Japan

*e-mail: keyem@kuhp.kyoto-u.ac.jp

Y. Ogawa, A. Sugawara

Department of Nephrology, Osaka Redcross Hospital, Osaka, Japan

Address correspondence to*: Kiyoshi Mori*

Department of Medicine and Clinical Science, Kyoto University Graduate School of Medicine

54 Shogoin Kawaharacho, Sakyoku, Kyoto 606-8507, Japan

e-mail: keyem@kuhp.kyoto-u.ac.jp

Abstract: 243 words. Total body length excluding abstract, acknowledgements, references, tables and figure legends: 3,964 words.

Number of tables and figures: 1 Table and 7 Figures. 47 references.

Abstract

Aims/hypothesis

Hyperlipidaemia is an independent risk factor for the progression of diabetic nephropathy, but its molecular mechanism remains elusive. We investigated in mice how diabetes and hyperlipidaemia cause renal lesions separately or in combination, and the involvement of toll-like receptor 4 (TLR4) in this process.

Methods

Diabetes was induced in wild-type (WT) and *Tlr4* knockout (KO) mice by intraperitoneal injection of streptozotocin (STZ). At 2 weeks after STZ injection, normal diet was substituted with high-fat diet (HFD). Functional and histological analysis was carried out 6 weeks later.

Results

As compared to treatment with STZ or HFD alone, treatment of WT mice with both STZ and HFD markedly aggravated nephropathy, as indicated by increase in albuminuria, mesangial expansion, and infiltration of macrophages and upregulation of pro-inflammatory and extracellular matrix-associated gene expression in glomeruli. In *Tlr4* KO mice, addition of HFD to STZ had almost no effects as to above parameters. Protein expression of S100a8, a potent ligand for Tlr4, was abundantly observed in macrophages infiltrating STZ-HFD WT glomeruli and in glomeruli of diabetic nephropathy patients. High glucose and fatty acid treatment synergistically upregulated *S100a8* gene expression in macrophages from WT mice, but not from KO. As putative downstream targets of Tlr4, phosphorylation of Irf3 was enhanced in kidneys of WT mice co-treated with STZ and HFD.

Conclusions/interpretation

Activation of S100a8/Tlr4 signaling was elucidated in an animal model of diabetic glomerular injury accompanied with hyperlipidaemia, which may provide novel therapeutic targets in progressive diabetic nephropathy.

Keywords: Diabetic Nephropathy, Glomerulus, High Fat Diet, Hyperlipidaemia, Macrophages, S100A8, TLR4

Abbreviations: ESRD, end-stage renal disease; HFD, high fat diet; KO, knockout; ND, normal diet; nSTZ, non-STZ; TG, triacylglycerol; STZ, streptozotocin; TLR, toll-like receptor; WT, wild-type

Introduction

Diabetic nephropathy is one of the most prevalent causes of end-stage renal disease (ESRD) [1]. Despite progress in pharmacological strategies to control diabetes, hypertension and other metabolic abnormalities, the number of patients entering into the stage of ESRD due to diabetic nephropathy remains extremely large, and development of new classes of treating reagents is expected eagerly [2]. During recent decades, the pathophysiology of diabetic nephropathy is becoming complex and serious because of coexisting life-style-related disorders such as hyperlipidaemia, hypertension and obesity [3]. In fact, hyperlipidaemia is an independent risk factor for the progression of diabetic nephropathy both in type 1 and type 2 diabetes [4, 5], but the underlying molecular mechanism remains elusive [6].

Toll-like receptors (TLRs) are a family of receptors playing a critical role in the innate immune system by activating proinflammatory signaling pathways in response to molecular patterns synthesized by microorganisms [7]. TLR4, one of the best-characterized TLRs, binds with lipopolysaccharide from gram-negative bacterial cell walls and with several endogenous ligands [7]. TLR4 also plays an important role in various kidney disorders, such as glomerulonephritis, renal ischemia and diabetic tubular inflammation [8-13], but the role of TLR4 in diabetic glomelular injury or hyperlipidaemia-induced kidney damage remains largely unknown.

In the current study, TLR4 and its novel endogenous ligand S100A8 emerged as candidate molecules involved in the progression of diabetic nephropathy by our microarray analysis performed in two different types of diabetic mouse models. Furthermore, we examined the effects of high-fat diet (HFD) feeding on streptozotocin (STZ)-induced diabetes in *Tlr4* knockout (KO) and wild-type (WT) mice in order to elucidate the mechanism for the progression of diabetic nephropathy caused by hyperlipidaemia.

Methods

Experimental animals

Male *Tlr4* KO [14] and WT mice with C57BL/6J genetic background were studied. For generation of a mouse model of diabetes complicated with hyperlipidaemia, 8-week-old mice were intraperitoneally injected with STZ (100mg/kg body weight in citrate buffer, pH 4.0; Sigma-Aldrich, St Louis, MO, USA) or vehicle for 3 consecutive days. After 2 weeks, normal diet (ND; NMF, 14.7 kJ/g [3.5 kcal/g], 13% of energy as fat; Oriental Yeast Co., Tokyo, Japan) was substituted with HFD (D12451, 19.7 kJ/g [4.7 kcal/g], 45% of energy as fat; Research Diets, New Brunswick, NJ, USA) in subgroups of animals, and all were killed for analysis at 8 weeks after STZ treatment. In another set of experiments, 8-week-old male *db/db* mice (in BKS genetic background; Japan Clea, Tokyo, Japan) were randomly assigned into ND or HFD (D12492, 21.8 kJ/g [5.2 kcal/g], 60% of energy as fat; Research Diets) groups and followed for 4 weeks. All animal experiments were conducted in accordance with the Guidelines for Animal Research Committee of Kyoto University Graduate School of Medicine.

Human biopsy samples

Human kidney samples obtained at renal biopsy carried out in our department were used for immunohistochemistry. The human study protocol was approved by the Ethical Committee on Human Research of Kyoto University Graduate School of Medicine. All participants gave written informed consent.

Measurement of metabolic parameters

Metabolic parameters were measured as described previously [15, 16]. Briefly, blood pressure was measured by indirect tail-cuff method (Muromachi Kikai, Tokyo, Japan). Urine samples were collected with metabolic cages, and urinary albumin was measured with competitive ELISA (Exocell, Philadelphia, PA, USA). Serum and urinary

creatinine levels were assayed by enzymatic method (SRL, Tokyo, Japan) [17]. Plasma glucose, triacylglycerol (TG) and total cholesterol levels were measured at ad libitum-fed conditions using enzymatic method (Wako Pure Chemicals, Osaka, Japan). Plasma insulin levels were measured by enzyme immunoassay (Morinaga, Tokyo, Japan). For measurement of tissue TG contents, lipids were extracted with isopropyl alcohol/heptane (1:1 vol./vol.) from frozen kidney samples. After evaporating the solvent, lipids were resuspended in 99.5% ethanol and TG contents were measured as described above.

Real-time quantitative RT-PCR

Total RNA was extracted with TRIzol reagent (Invitrogen, Carlsbad, CA, USA) and cDNA in each sample was synthesized by High Capacity cDNA Reverse Transcription Kit (Applied Biosystems, Foster City, CA, USA) from mouse kidneys and glomeruli that were isolated by graded sieving method [18, 19]. TaqMan real-time PCR was performed using Premix Ex Taq (Takara Bio, Otsu, Japan) and StepOnePlus Real Time PCR System (Applied Biosystems, Foster City, CA, USA). See electronic supplementary material (ESM) Table 1 for primer and probe sequences. Expression levels of all genes were normalized by *Gapdh* (internal control) levels. Mean expression level in whole kidney of WT, non-treated control mice was arbitrarily defined as 1.0.

Histological analysis

Periodic acid–Schiff (PAS) staining of mesangial area and immunohistochemistry of S100a8 (requiring antigen retrieval by citrate buffer) and Mac-2 (or Lgals3)[18] were carried out using kidney sections (thickness 4 μm) fixed with 4% buffered paraformaldehyde. Nuclei were counterstained with hematoxylin. All primary antibodies used in this study are shown in ESM Table 2. For double staining, primary antibody for S100a8 was visualized with DyLight-conjugated secondary antibody (Takara Bio, Otsu, Japan). Immunofluorescence of Podocin (or

Nphs2) was performed with snap frozen cryostat sections (4 μm), pretreated with cold acetone and 0.1% Triton-X100, and with primary and FITC-labelled secondary antibodies. Photos were taken by a fluorescence microscope (IX81-PAFM; Olympus, Tokyo, Japan). Mesangial and Podocin-positive areas of more than 10 glomeruli from the outer cortex were measured quantitatively to obtain an average for each mouse using MetaMorph 7.5 software (Molecular Devices, Downingtown, PA, USA). Formalin-fixed, snap-frozen sections (10 μm) were stained with Oil Red O to evaluate lipid droplet-positive areas.

Microarray analysis

Two different types of diabetic model mice were employed for microarray analysis. Male A-ZIP/F-1 heterozygous transgenic mice and control male FVB/N littermates were used at 10 months of age, when A-ZIP/F-1 mice exhibited diabetic nephropathy with massive proteinuria [20]. The other model was STZ-induced, insulin-dependent, diabetic C57BL/6J male mice (Japan Clea, Tokyo, Japan) whose diabetes was induced at 9 weeks of age by single intraperitoneal injection of STZ (180 mg/kg) and analyzed 8 weeks later. We essentially followed the procedures described in detail in the GeneChip Eukaryotic Target Preparation & Hybridization Manual (Affymetrix, Santa Clara, CA, USA). In brief, cDNA was synthesized and biotin-labelled cRNA was produced through in vitro transcription labelling Kit (Affymetrix). Fragmented cRNA was hybridized to GeneChip Mouse Genome 430 2.0 Array (Affymetrix) at 45°C for 16 h. The samples were washed and stained according to the manufacturer’s protocol on GeneChip Fludisc Station 450 (Affymetrix) and scanned on GeneChip Scanner 3000 (Affymetrix).

PCR Array analysis

To eliminate contaminating genomic DNA, total RNA extracted from kidney samples was purified using RNeasy

Mini Kit (QIAGEN Sciences, Maryland, MD, USA). First-strand cDNA was synthesized from total RNA using RT2 first-strand kit (SABiosciences, Frederick, MD, USA). Mouse TLR-signaling pathway RT2 Profiler PCR plate (PAMM-018, SABiosciences) and StepOnePlus were used for amplification of cDNA. 96-well plates containing gene-specific primer sets for 84 relevant TLR pathway genes, 5 housekeeping genes, and 2 negative controls were used. The cycle threshold (CT) was determined for each sample and normalized to the average CT of the 5 housekeeping genes. Comparative delta-CT method (SABiosciences) was used to calculate relative gene expression.

Western blot analysis

Proteins extracted from kidney samples were separated by SDS-PAGE, transferred onto PVDF membranes, incubated with primary antibodies and detected with peroxidase-conjugated secondary antibodies and chemiluminescence [19]. Gapdh was used as an internal control.

Cultured macrophages

Palmitate (Sigma-Aldrich) was solubilized in ethanol, and combined with fatty acid-free, low endotoxin, bovine serum albumin (Sigma-Aldrich) at a molar ratio of 10: 1 in serum-free medium. Polymyxin B (10 μg/ml, Nacalai Tesque, Kyoto, Japan) was added to each well to minimize contamination of endotoxin. Bone marrow-derived macrophages were generated from mice as described previously [21]. Briefly, following lysis of red blood cells, bone marrow cells were resuspended in medium containing 20% fetal calf serum and 50 ng/ml recombinant human M-CSF, and cultured at 37°C in 5% CO_2 atmosphere. On day 6, medium was replaced with fresh one containing 5.6 mM or 25 mM glucose. On day 7, macrophages were incubated with palmitate or vehicle for 24 h. Total RNA from cells was extracted with RNeasy Mini Kit, and mRNA expression levels of *S100a8* and *Tlr4* were

determined by TaqMan real-time RT-PCR.

Statistical analysis

Data are expressed as means±SEM. Differences between multiple groups were assessed by two-way factorial ANOVA with Bonferroni's post test. Comparison between two groups was carried out by unpaired Student's t test. Statistical significance was defined as $p<0.05$.

Results

Changes of metabolic parameters and albuminuria in wild-type diabetic mice given fat-rich diet

Metabolic parameters of non-STZ (nSTZ)-HFD, STZ-ND, STZ-HFD and control nSTZ-ND groups in WT mice are shown in Table 1. HFD treatment (as compared to ND) in nSTZ mice caused significant elevation of body weight, plasma glucose, insulin, TG and total cholesterol levels. STZ treatment (compared to nSTZ) in ND mice caused significant body weight loss and significant elevation of plasma glucose, TG and total cholesterol levels. Treatment of STZ mice with HFD resulted in large exacerbation of hypertriglyceridaemia (by 2.3-fold) without significant changes in other, above-mentioned parameters (Table 1). Consistently, renal lipid deposition in STZ-HFD mice was markedly increased as compared to STZ-ND mice (Fig. 1a, b). Blood pressures were not significantly different among the four treatment groups (Table 1).

Concerning albuminuria, one of the representative abnormalities which characterize diabetic nephropathy [2], albumin excretion in STZ-ND was elevated by 2.3-fold at 8 weeks as compared to nSTZ-ND mice (Fig. 1c). Addition of HFD to STZ mice further enhanced albuminuria approximately by two-fold. To investigate podocyte injury, we investigated whether Podocin protein expression is decreased in glomeruli of STZ-HFD mice [19]. Glomerular Podocin expression was significantly reduced in STZ-ND compared to nSTZ-ND and its expression was lowest in STZ-HFD (Fig. 1e, f). Also in obese, type 2 diabetic *db/db* mice, albuminuria was exaggerated by HFD (ESM Fig. 1). To summarize, combinatory treatment of WT mice with HFD and STZ resulted in marked enhancement of hypertriglyceridaemia, renal lipid deposition, podocyte damage and albumin excretion.

Gene expression analysis of pro-inflammatory and extracellular matrix-associated genes in whole kidney and

glomeruli and histological examination

We measured mRNA levels of pro-inflammatory and extracellular matrix (ECM)-associated genes both in whole kidney and isolated glomeruli (Fig. 2, ESM Table 3). The former genes included *Mcp1* (or *Ccl2*, encoding monocyte chemoattractant protein-1), *F4/80* (Emr1), *Cd68*, *Tnfa* (tumor necrosis factor α), *Pai1* (plasminogen activator inhibitor-1) and *Il1b* (interleukin-1 β); and the latter were *Tgfb1* (transforming growth factor β1), *Fn* (fibronectin), *Col4a3* (type IV collagen alpha 3 chain), *Ctgf* (connective tissue growth factor) and *Mmp2* (matrix metalloproteinase 2). We found that expression levels of these genes in glomeruli and whole kidney were mildly elevated in WT STZ-ND compared to WT nSTZ-ND mice, in general (Fig. 2, ESM Table 3). Furthermore, gene expression levels were further upregulated in WT STZ-HFD animals. Of note, differences between nSTZ-HFD and nSTZ-ND groups were negligible (Fig. 2). Histological analysis also showed that Mac-2^{+}-macrophage infiltration into glomeruli (Fig. 3a) and renal interstitium (ESM Fig. 2) and glomerular mesangial expansion (Fig. 3b) in STZ-HFD were markedly larger than those in STZ-ND mice.

Screening of candidate genes involved in pathogenesis of diabetic nephropathy

To identify candidate molecules potentially involved in the pathophysiology of diabetic nephropathy, we analyzed gene expression profiles of diabetic mouse glomeruli by microarray (ESM Table 4). We decided to compare 2 types of diabetic nephropathy from STZ-induced and A-ZIP/F-1 lipoatrophic diabetes mice. We selected commonly regulated genes to minimize interference from renal toxicity of STZ, from genetic background [22] and from direct insulin or leptin target molecules [23]. List of genes commonly upregulated in these 2 models included pro-inflammatory and ECM-associated genes and also ones encoding TLRs (ESM Table 4). Since pairs of cell surface receptors and their ligands provide attractive seeds for future therapeutic targets, we focused upon Tlr4,

whose glomerular expression levels were elevated by 1.7-fold by STZ and 5.8-fold in A-ZIP/F-1 as compared to each control by microarray. We further examined the expression of molecules reported to be endogenous ligands for Tlr4 [7], and identified S100a8 (or myeloid-related protein 8, Mrp8) and S100a9 (Mrp14) [24], whose glomerular expressions were commonly upregulated in 2 models of diabetic nephropathy by microarray (ESM Table 4). Upregulation of *Tlr4* and *S100a8* gene expression in glomeruli of STZ and A-ZIP/F-1 mice were confirmed by quantitative RT-PCR (ESM Fig. 3a, b). Moreover, in STZ-HFD mice, expression of these genes was further potentiated as compared to other groups such as STZ-ND and nSTZ-HFD, especially in glomeruli (Fig. 4a), but not in whole kidney (ESM Fig. 4). On the other hand, expressions of other endogenous ligands for Tlr4, such as Hmgb1 (high mobility group box 1), were not largely and simultaneously upregulated in STZ and A-ZIP/F-1 mice as compared to their respective controls by microarray (ESM Table 4) or by quantitative RT-PCR (ESM Fig. 3c, d).

Expression of S100a8 protein in diabetic kidney

We performed immunohistochemical analyses of S100a8 protein in the kidneys both in STZ-HFD mice and human biopsy samples. In mice, abundant expression of S100a8 protein, in a punctate pattern, was observed predominantly in glomeruli of WT STZ-HFD mice, while S100a8 expression was much less in glomeruli of nSTZ-ND, nSTZ-HFD and STZ-ND groups (Fig. 4b, ESM Fig. 5). S100a8 protein was also expressed in the interstitium of STZ-HFD mice but less abundantly compared to glomerular expression. Double immunostaining revealed that 86% of S100a8 signals co-localized with macrophage marker Mac-2 in glomeruli of STZ-HFD mice (Fig. 4c). In humans, S100A8 was abundantly expressed in glomeruli of patients with diabetic nephropathy, but not obviously in glomeruli of minor glomerular abnormality or minimal change nephrotic syndrome cases (Fig.

5).

Effects of Tlr4 defect upon STZ-HFD mice and upon bone marrow-derived macrophages

To elucidate a functional role played by Tlr4 in the progression of diabetic nephropathy accelerated by diet-induced hyperlipidaemia, we investigated effects of STZ and HFD in *Tlr4* KO mice. In baseline nSTZ-ND conditions, KO mice showed significantly heavier body weights compared to WT mice, which was paralleled by mildly elevated plasma levels of glucose, insulin, TG and total cholesterol in KO mice (Table 1). Plasma glucose levels in KO nSTZ-HFD mice were slightly lower compared to their WT counterparts. These findings are consistent with previous observations indicating that, as compared to WT mice, *Tlr4* KO mice are prone to accumulation of fat but resistant to development of insulin resistance when challenged by HFD [25, 26]. When STZ-HFD conditions were compared between KO and WT mice, the levels of plasma glucose and total cholesterol and renal lipid deposition were similar among the genotypes and plasma TG levels tended to be higher in KO than WT mice (Table 1, Fig. 1b). On the other hand, exacerbation of albuminuria and suppression of glomerular Podocin protein expression resulting from HFD treatment in WT STZ mice were all largely blunted in KO STZ animals (Fig. 1c-f). Additionally, infiltrated macrophage counts in glomeruli and renal interstitium and mesangial expansion were remarkably smaller in KO STZ-HFD than those in WT STZ-HFD mice (Fig. 3, ESM Fig. 2). Furthermore, upregulation of pro-inflammatory (*Mcp1* and *Pai1*), pro-fibrotic (*Fn* and *Ctgf*), *S100a8* and *S100a9* gene expression and S100a8-positive cell counts caused by HFD treatment in glomeruli of WT STZ mice were almost completely abolished in KO STZ mice (Fig. 2, Fig. 4a, b, ESM Fig. 5). These findings indicate that, despite similar degrees of metabolic abnormalities caused by diabetes and hyperlipidaemia, *Tlr4* KO developed much less severe renal lesions as compared to WT mice.

With regard to comparison between WT and *Tlr4* KO mice treated with STZ alone (STZ-ND mice), urinary albumin excretion (Fig. 1c, d), glomerular Podocin expression (Fig. 1e, f), glomerular gene expression of *Mcp1*, *Pai1*, *Fn*, *Ctgf*, *S100a8* and *S100a9* (Fig. 2, Fig. 4a), and glomerular macrophage infiltration (Fig. 3a) were all similar among two genotypes, suggesting that *Tlr4* does not strongly participate in early and mild changes of diabetic nephropathy. Concerning HFD alone treatment (nSTZ-HFD mice), there was no significant difference in urinary albumin excretion and glomerular Podocin expression between WT and KO mice (Fig. 1c-f), while glomerular *S100a9* gene expression (Fig. 4a) and glomerular macrophage infiltration (Fig. 3a) were significantly attenuated in KO as compared to WT, suggesting that treatment solely with HFD significantly activated circulating macrophages in WT mice but Tlr4-mediated signal in nSTZ-HFD mice was not sufficient to cause functional changes in glomeruli.

To gain insights concerning how combination of diabetes and hyperlipidaemia resulted in markedly enhanced migration of macrophages into glomeruli, we examined bone marrow-derived macrophages. We focused attention upon expression of a potent Tlr4 ligand, S100a8 [24]. Treatment of WT macrophages with a fatty acid, palmitate, induced *S100a8* mRNA upregulation when the cells were cultured in high glucose conditions, but upregulation was not observed under low glucose conditions (Fig. 6a). Furthermore, induction of *S100a8* expression by palmitate in high glucose-treated macrophages did not occur in cells from *Tlr4* KO animals (Fig. 6b). High glucose treatment slightly increased *Tlr4* expression in WT macrophages (Fig. 6c).

Tlr4 signaling in the kidney of STZ-HFD model

To examine Tlr4-downstream signaling cascade, we performed Western blot analyses of key adaptor proteins and transcription factors which have been reportedly classified into Myd88-dependent, Trif (TIR-domain-containing

adapter-inducing interferon-β)-dependent or common pathways (Fig. 7a) [7], using whole kidney lysate. Treatment of WT STZ mice with HFD was associated with increased phosphorylation of Ikb (inhibitor κB) and Jnk (c-Jun N-terminal kinase) in common pathway, and with increased phosphorylation of Irf3 (interferon regulatory factor 3) in Trif-dependent pathway, but neither with increased protein expression of Traf6 (TNF receptor-associated factor 6) nor with increased phosphorylation of Irak (interleukin-1 receptor–associated kinase) in Myd88-dependent pathway (Fig. 7b, c). PCR-array analysis, which allows simultaneous evaluation of relevant genes involved in the signaling cascades of Tlr1-Tlr9, confirmed that in WT STZ-HFD kidneys, Trif-dependent pathway-inducible genes (*Cxcl10*, *Ifnb1* [encoding interferon β1] and *Cd80*) and common pathway-inducible genes (*Mcp1*) were highly upregulated, but genes involved in Myd88-dependent pathway (*Cd14*, *Ly96* [encoding MD-2], and *Traf6*) were not changed compared to WT STZ-ND kidneys (ESM Table 5). Furthermore, disruption of *Tlr4* gene markedly blocked the activation of putative Tlr4 downstream signaling cascade in STZ-HFD mice (Fig. 7b, c, ESM Table 5).

Discussion

In the present study, we have revealed that combinatory treatment of WT mice with STZ and HFD synergistically aggravated renal lesions, which were indicated by enhancement of albuminuria, macrophage infiltration, mesangial expansion and pro-inflammatory/ECM-associated gene induction in glomeruli. These changes were accompanied with upregulation of a Tlr4 ligand S100a8 and activation of putative Trif-dependent pathway downstream of Tlr4. In *Tlr4* KO mice, addition of HFD to STZ had almost no effects upon kidney damage, suggesting that Tlr4 plays an important role in exacerbation of diabetic nephropathy by hyperlipidaemia.

Of note, treatment with STZ alone caused similar and mild renal changes in WT and KO mice, suggesting that Tlr4 signal may not significantly participate in the onset of diabetic nephropathy at 8 weeks after STZ injection [13]. On the other hand, WT mice fed with HFD (nSTZ-HFD) exhibited significantly larger *S100a9* gene expression and more macrophage infiltration in glomeruli as compared to KO mice, but these effects were not reflected to differences in other parameters of renal lesions, suggesting that macrophage activation in nSTZ-HFD mice may require longer observation periods than ones in this study to be functionally relevant.

Here, to study the effects of HFD upon diabetes, we took advantage to use lean, type 1 diabetes model to avoid complexity due to alteration of insulin resistance and fat accumulation by HFD or by *Tlr4* gene disruption in type 2 diabetes model [19, 20]. HFD-induced and hypertriglyceridemia-associated renal injury observed in this study may have been caused through activation of Tlr4 by free fatty acids [25, 26], oxidized LDL [27], or TG-rich lipoproteins [6]. Previous studies have proposed that, by direct lipotoxicity upon tubular epithelial cells, diet-induced obesity alone is sufficient to cause inflammatory and fibrotic changes in the whole kidney preparations through expression of Cd36 and Srebp1c (sterol regulatory element-binding protein-1c) [28-30]. In

the present study, however, treatment of WT mice solely with HFD resulted in very mild renal lesions, likely because we used diet with less fat content and studied for a shorter period of time compared to earlier reports [28-30]. Furthermore, HFD increased glomerular *Cd36* mRNA expression but STZ-induced diabetes reduced it, and glomerular *Srebp1c* expression was decreased both by HFD and STZ (ESM Fig. 6), indicating that HFD-induced exacerbation of diabetic nephropathy cannot be explained by upregulation of Cd36 or Srebp1c.

S100a8 forms a heterodimer with S100a9, and the complex is one of the most powerful, endogenous ligands for Tlr4, which is essential in full activation of macrophages and other leukocytes, by a positive feedback loop, during endotoxin-induced shock and vascular and autoimmune disorders [24, 31, 32]. Tlr4 signaling also plays an important role in the development of various kidney diseases, yet the role of Tlr4 in diabetic glomerulopathy or hyperlipidaemia-induced kidney damage have remained to be elucidated [8-13]. Recently, Burkhardt et al. and Bouma et al. reported that serum S100A8/A9 complex concentrations were elevated in patients with diabetes [33, 34]. In our study, S100a8 protein was abundantly expressed in glomeruli of mice given STZ and HFD and also in glomeruli of patients with diabetic nephropathy, and was mainly expressed by macrophages. Furthermore, we found that high glucose and free fatty acid treatments, when combined, markedly upregulated *S100a8* expression in WT macrophages, but not in *Tlr4* KO macrophages. These findings suggest that expression of S100a8 is not just an indicator of systemic inflammation but may play a pathogenic role in deterioration of diabetic nephropathy. Functional analysis of S100a8 protein expression in diabetic mice is currently underway in our lab. On the other hand, candidate Tlr4-expressing cells in diabetic kidney include macrophages, podocytes, mesangial and tubular epithelial cells [8, 9]. So far, we could not obtain reliable findings by immunohistochemistry using commercially-available antibodies for Tlr4, and are now trying other methods. Of

note, upregulation of *S100a8* gene expression by HFD in STZ mice was also observed in the liver and aorta, suggesting that effects of these treatments are not specifically targeted to the kidney but are systemic (ESM Fig. 6). Hmgb1 is one of endogenous ligands of Tlr4 [9], and Ager (advanced glycosylation end product-specific receptor or RAGE) is one of S100a8 receptors so far identified [35]. Although mRNA expressions of these molecules in glomeruli were not upregulated in diabetic mice of this study (ESM Fig. 3, ESM Table 4), we cannot exclude a possibility that they are involved in hyperlipidaemia-induced renal injury.

Macrophage has been presumed to be a critical mediator of diabetic nephropathy [36-38], and blockade of the MCP-1/CC chemokine receptor 2 system in diabetic mice leads to reduced albuminuria, mesangial expansion and macrophage infiltration [39-42]. Secretory factors from macrophages may cause histological and functional changes in glomeruli. For instance, Tgfb1 (transforming growth factor β1) and Mcp1, induced in surrounding cells by or secreted directly by activated macrophages, have been shown to upregulate Ctgf expression [43] and increase albumin permeability in cultured podocytes [44-46], and we have recently reported that overexpression of Ctgf specifically in podocytes is sufficient to worsen diabetic nephropathy [19].

Downstream signaling of Tlr4 have been divided into Myd88-dependent and Trif–dependent pathways, and they lead to early- and late-phase Nfkb (NF-κB) activation, respectively [7]. In addition, endocytosed Tlr4 activates Trif-dependent pathway [47]. It is interesting if pathologically accumulated lipids in endosomes of macrophages can cause chronic inflammation via Trif-dependent pathway in the kidney of STZ-HFD mice. Here, in STZ-HFD kidneys, we observed increase of Irf3 protein phophophorylation and *Cxcl10*, *Ifnb1* and *Cd80* mRNA expression reported to be in Trif-dependent pathway, but experiments blocking Trif activity is required to demonstrate Trif-dependency of the process.

In conclusion, we have elucidated a novel mechanism of hyperlipidaemia-induced renal damage in diabetic conditions in a Tlr4-dependent manner, which appears to involve the activation of S100a8/Tlr4 signaling pathway in glomeruli. Further investigation is required to see whether this signaling cascade is relevant in the progression of nephropathy in diabetic patients.

Acknowledements

We acknowledge S. Akira (WPI Immunology Frontier Research Center, Osaka University, Suita, Japan) for kindly providing us with *Tlr4* KO mice. This work was supported in part by Grant-in-Aid for Diabetic Nephropathy Research (K. Mori), research grants from Japanese Ministry of Education, Culture, Sports, Science and Technology (T. Kuwabara, K. Mori and M. Mukoyama) and from Smoking Research Foundation (M. Mukoyama). We gratefully acknowledge Yuri Ogawa and A. Yamamoto and other lab members for assistance.

Contribution statement

All authors have contributed to the conception and design, or analysis and interpretation of data, and drafting the article or revising it critically for important intellectual content, and have given final approval of the version to be published.

Duality of interest

The authors declare that there is no duality of interest associated with this manuscript.

References

1. Maisonneuve P, Agodoa L, Gellert R et al (2000) Distribution of primary renal diseases leading to end-stage renal failure in the United States, Europe, and Australia/New Zealand: results from an international comparative study. Am J Kidney Dis 35:157-165

2. Decleves AE, Sharma K (2010) New pharmacological treatments for improving renal outcomes in diabetes. Nat Rev Nephrol 6:371-380

3. El-Atat FA, Stas SN, McFarlane SI, Sowers JR (2004) The relationship between hyperinsulinemia, hypertension and progressive renal disease. J Am Soc Nephrol 15:2816-2827

4. Perkins BA, Ficociello LH, Silva KH, Finkelstein DM, Warram JH, Krolewski AS (2003) Regression of microalbuminuria in type 1 diabetes. N Engl J Med 348:2285-2293

5. Ravid M, Brosh D, Ravid-Safran D, Levy Z, Rachmani R (1998) Main risk factors for nephropathy in type 2 diabetes mellitus are plasma cholesterol levels, mean blood pressure, and hyperglycemia. Arch Intern Med 158:998-1004

6. Rutledge JC, Ng KF, Aung HH, Wilson DW (2010) Role of triglyceride-rich lipoproteins in diabetic nephropathy. Nat Rev Nephrol 6:361-370

7. Akira S, Takeda K (2004) Toll-like receptor signalling. Nat Rev Immunol 4:499-511

8. Brown HJ, Lock HR, Wolfs TG, Buurman WA, Sacks SH, Robson MG (2007) Toll-like receptor 4 ligation on intrinsic renal cells contributes to the induction of antibody-mediated glomerulonephritis via CXCL1 and CXCL2. J Am Soc Nephrol 18:1732-1739

9. Wu H, Chen G, Wyburn KR et al (2007) TLR4 activation mediates kidney ischemia/reperfusion

injury. J Clin Invest 117:2847-2859

10. Zhang B, Ramesh G, Uematsu S, Akira S, Reeves WB (2008) TLR4 signaling mediates inflammation and tissue injury in nephrotoxicity. J Am Soc Nephrol 19:923-932

11. Liu B, Yang Y, Dai J et al (2006) TLR4 up-regulation at protein or gene level is pathogenic for lupus-like autoimmune disease. J Immunol 177:6880-6888

12. Kruger B, Krick S, Dhillon N et al (2009) Donor Toll-like receptor 4 contributes to ischemia and reperfusion injury following human kidney transplantation. Proc Natl Acad Sci U S A 106:3390-3395

13. Lin M, Yiu WH, Wu HJ et al (2012) Toll-like receptor 4 promotes tubular inflammation in diabetic nephropathy. J Am Soc Nephrol 23:86-102

14. Hoshino K, Takeuchi O, Kawai T et al (1999) Cutting edge: Toll-like receptor 4 (TLR4)-deficient mice are hyporesponsive to lipopolysaccharide: evidence for TLR4 as the Lps gene product. J Immunol 162:3749-3752

15. Kuwabara T, Mori K, Mukoyama M et al (2009) Urinary neutrophil gelatinase-associated lipocalin levels reflect damage to glomeruli, proximal tubules, and distal nephrons. Kidney Int 75:285-294

16. Kusakabe T, Tanioka H, Ebihara K et al (2009) Beneficial effects of leptin on glycaemic and lipid control in a mouse model of type 2 diabetes with increased adiposity induced by streptozotocin and a high-fat diet. Diabetologia 52:675-683

17. Jung K, Wesslau C, Priem F, Schreiber G, Zubek A (1987) Specific creatinine determination in

laboratory animals using the new enzymatic test kit "Creatinine-PAP". J Clin Chem Clin Biochem 25:357-361

18. Suganami T, Mukoyama M, Sugawara A et al (2001) Overexpression of brain natriuretic peptide in mice ameliorates immune-mediated renal injury. J Am Soc Nephrol 12:2652-2663

19. Yokoi H, Mukoyama M, Mori K et al (2008) Overexpression of connective tissue growth factor in podocytes worsens diabetic nephropathy in mice. Kidney Int 73:446-455

20. Suganami T, Mukoyama M, Mori K (2005) Prevention and reversal of renal injury by leptin in a new mouse model of diabetic nephropathy. FASEB J 19:127-129

21. Suganami T, Yuan X, Shimoda Y et al (2009) Activating transcription factor 3 constitutes a negative feedback mechanism that attenuates saturated Fatty acid/toll-like receptor 4 signaling and macrophage activation in obese adipose tissue. Circ Res 105:25-32

22. Qi Z, Fujita H, Jin J et al (2005) Characterization of susceptibility of inbred mouse strains to diabetic nephropathy. Diabetes 54:2628-2637

23. Vaisse C, Halaas JL, Horvath CM, Darnell JE, Jr., Stoffel M, Friedman JM (1996) Leptin activation of Stat3 in the hypothalamus of wild-type and ob/ob mice but not db/db mice. Nat Genet 14:95-97

24. Vogl T, Tenbrock K, Ludwig S et al (2007) Mrp8 and Mrp14 are endogenous activators of Toll-like receptor 4, promoting lethal, endotoxin-induced shock. Nat Med 13:1042-1049

25. Suganami T, Mieda T, Itoh M, Shimoda Y, Kamei Y, Ogawa Y (2007) Attenuation of obesity-induced adipose tissue inflammation in C3H/HeJ mice carrying a Toll-like receptor 4

mutation. Biochem Biophys Res Commun 354:45-49

26. Shi H, Kokoeva MV, Inouye K, Tzameli I, Yin H, Flier JS (2006) TLR4 links innate immunity and fatty acid-induced insulin resistance. J Clin Invest 116:3015-3025

27. Xu XH, Shah PK, Faure E et al (2001) Toll-like receptor-4 is expressed by macrophages in murine and human lipid-rich atherosclerotic plaques and upregulated by oxidized LDL. Circulation 104:3103-3108

28. Kume S, Uzu T, Araki S et al (2007) Role of altered renal lipid metabolism in the development of renal injury induced by a high-fat diet. J Am Soc Nephrol 18:2715-2723

29. Okamura DM, Pennathur S, Pasichnyk K et al (2009) CD36 regulates oxidative stress and inflammation in hypercholesterolemic CKD. J Am Soc Nephrol 20:495-505

30. Jiang T, Wang Z, Proctor G et al (2005) Diet-induced obesity in C57BL/6J mice causes increased renal lipid accumulation and glomerulosclerosis via a sterol regulatory element-binding protein-1c-dependent pathway. J Biol Chem 280:32317-32325

31. Croce K, Gao H, Wang Y et al (2009) Myeloid-related protein-8/14 is critical for the biological response to vascular injury. Circulation 120:427-436

32. Loser K, Vogl T, Voskort M et al (2010) The Toll-like receptor 4 ligands Mrp8 and Mrp14 are crucial in the development of autoreactive CD8+ T cells. Nat Med 16:713-717

33. Burkhardt K, Schwarz S, Pan C et al (2009) Myeloid-related protein 8/14 complex describes microcirculatory alterations in patients with type 2 diabetes and nephropathy. Cardiovasc Diabetol 8:10

34. Bouma G, Lam-Tse WK, Wierenga-Wolf AF, Drexhage HA, Versnel MA (2004) Increased serum levels of MRP-8/14 in type 1 diabetes induce an increased expression of CD11b and an enhanced adhesion of circulating monocytes to fibronectin. Diabetes 53:1979-1986

35. Yamamoto Y, Kato I, Doi T et al (2001) Development and prevention of advanced diabetic nephropathy in RAGE-overexpressing mice. J Clin Invest 108:261-268

36. Furuta T, Saito T, Ootaka T et al (1993) The role of macrophages in diabetic glomerulosclerosis. Am J Kidney Dis 21:480-485

37. Sassy-Prigent C, Heudes D, Mandet C et al (2000) Early glomerular macrophage recruitment in streptozotocin-induced diabetic rats. Diabetes 49:466-475

38. Usui HK, Shikata K, Sasaki M et al (2007) Macrophage scavenger receptor-a-deficient mice are resistant against diabetic nephropathy through amelioration of microinflammation. Diabetes 56:363-372

39. Chow FY, Nikolic-Paterson DJ, Ozols E, Atkins RC, Rollin BJ, Tesch GH (2006) Monocyte chemoattractant protein-1 promotes the development of diabetic renal injury in streptozotocin-treated mice. Kidney Int 69:73-80

40. Chow FY, Nikolic-Paterson DJ, Ma FY, Ozols E, Rollins BJ, Tesch GH (2007) Monocyte chemoattractant protein-1-induced tissue inflammation is critical for the development of renal injury but not type 2 diabetes in obese db/db mice. Diabetologia 50:471-480

41. Kanamori H, Matsubara T, Mima A et al (2007) Inhibition of MCP-1/CCR2 pathway ameliorates the development of diabetic nephropathy. Biochem Biophys Res Commun 360:772-777

42. Sayyed SG, Ryu M, Kulkarni OP et al (2011) An orally active chemokine receptor CCR2 antagonist prevents glomerulosclerosis and renal failure in type 2 diabetes. Kidney Int 80:68-78

43. Yokoi H, Mukoyama M, Sugawara A et al (2002) Role of connective tissue growth factor in fibronectin expression and tubulointerstitial fibrosis. Am J Physiol Renal Physiol 282:F933-942

44. Takano Y, Yamauchi K, Hayakawa K et al (2007) Transcriptional suppression of nephrin in podocytes by macrophages: roles of inflammatory cytokines and involvement of the PI3K/Akt pathway. FEBS Lett 581:421-426

45. Lee EY, Chung CH, Khoury CC et al (2009) The monocyte chemoattractant protein-1/CCR2 loop, inducible by TGF-beta, increases podocyte motility and albumin permeability. Am J Physiol Renal Physiol 297:F85-94

46. Kwoh C, Shannon MB, Miner JH, Shaw A (2006) Pathogenesis of nonimmune glomerulopathies. Annu Rev Pathol 1:349-374

47. Kagan JC, Su T, Horng T, Chow A, Akira S, Medzhitov R (2008) TRAM couples endocytosis of Toll-like receptor 4 to the induction of interferon-beta. Nat Immunol 9:361-368

Table 1

Metabolic data of WT and *Tlr4* KO mice at 8 weeks after STZ injection

	WT				KO			
	nSTZ-ND	nSTZ-HFD	STZ-ND	STZ-HFD	nSTZ-ND	nSTZ-HFD	STZ-ND	STZ-HFD
Number of animals	6	4	8	11	4	4	5	8
Body weight (g)	27.7±1.0	33.7±0.5**	20.0±0.9**	22.1±0.5**###	34.9±2.4$	39.6±1.4$	22.0±1.3**	23.3±0.6***###
Blood pressure (mmHg)								
Systolic	101±2	104±2	98±1	100±1	103±2	103±2	96±1*	101±2
Diastolic	56±2	57±3	52±2	56±2	55±1	57±2	50±1*	53±1
Kidney weight (%body weight)	0.5±0.0	1.0±0.0**	1.7±0.1**	1.8±0.1**###	1.0±0.1$$$	2.2±0.2***$$	1.9±0.2***	1.9±0.1***
Plasma glucose (mmol/l)	9.5±1.6	14.0±0.4*	40.0±3.9**	32.9±1.8**#	10.4±1.1	12.7±2.3	36.0±7.7*	31.8±2.3***##
HbA1c (%)	3.4±0.1	5.3±0.1**	9.6±0.6**	9.9±0.5**#	3.0±0.3	4.9±0.2**	9.4±1.1**	10.3±0.3***###
Plasma insulin (pmol/l)	133 ±16	256±21**	10±2**	12±2**###	238±43	336±33	12±5**	12±5**###
Plasma triacylglycerol (mmol/l)	0.99±0.02	1.20±0.03**	2.36±1.01*	5.48±1.56*#	1.74±0.32	1.42±0.11	3.12±1.56	7.64±1.58**##
Plasma total cholesterol (mmol/l)	1.5±0.4	3.4±0.3*	5.1±0.8*	5.2±0.5**	1.9±0.4	3.4±0.2*	3.8±0.6*	5.9±0.4**##†
Serum creatinine (μmol/l)	8.0±1.8	8.8±0.1	10.6±0.9	15.9±5.3	8.8±0.1	8.0±0.1$$	10.6±1.8	8.0±0.1

Data are means±SEM. Blood was collected at *ad libitum* feeding conditions. nSTZ, non-STZ; ND, normal diet; HFD, high fat diet. *$p<0.05$ vs. nSTZ-ND. $^{\#}p<0.05$ vs. nSTZ-HFD. $^{\dagger}p<0.05$ vs. STZ-ND. $^{\$}p<0.05$ vs. similarly treated group of WT. Two symbols, $p<0.01$; three symbols, $p<0.001$.

Figure legends

Fig. 1

Treatment of STZ diabetic mice with high fat diet (HFD) worsens renal injury in WT but not in *Tlr4* KO mice. (a, b) Addition of HFD to STZ mice causes similar degrees of Oil Red O^{+}-lipid droplet deposition in WT (open bars) and KO mice (solid bars) at 16 weeks of age. Magnification, 4x. ND, normal diet. Data are means±SEM. *n*=5. ***p< 0.001. (c) Time course of urinary albumin levels normalized with urinary creatinine levels in WT (c) and *Tlr4* KO mice (d). Circles, nSTZ-ND; triangles, nSTZ-HFD; squares, STZ-ND; rhomboids, STZ-HFD. W, weeks after STZ injection. *n*=6-10. $^{\dagger}p$<0.05 vs. WT STZ-ND, $^{\$}p$<0.05 vs. WT STZ-HFD calculated by area under the curve. (e, f) Immunofluorescence analysis of glomerular Podocin expression. White bars, WT; black bars, KO. *n*=4-6. *p<0.05, **p<0.01, ***p<0.001. $^{\$}p$<0.05 for similarly treated KO vs. WT.

Fig. 2

Treatment with STZ and HFD synergistically upregulates inflammatory and extracellular matrix-associated gene expression in glomeruli of WT mice by real-time RT-PCR, but effects of HFD are largely blunted in *Tlr4* KO mice. White bars, WT; black bars, KO. Data are means±SEM. *n*=4-11. *p<0.05, **p<0.01, ***p<0.001.

Fig. 3

Glomerular macrophage infiltration and mesangial matrix accumulation are markedly enhanced in WT mice co-treated with STZ and HFD, but not in *Tlr4* KO mice. (a) Macrophage number per glomerular section determined by Mac-2 immunostaining (arrows). Magnification, 40x. Data are means±SEM. *n*=4-5. (b) Glomelular mesangial area determined by PAS staining (purple). Magnification, 20x. *n*=4-6. White bars, WT; black bars, KO. **p<0.01. ***p<0.001. $^{\$}p$<0.05, $^{\$\$}p$<0.01 for similarly treated KO vs. WT.

Fig. 4

Glomelular expression of *Tlr4*, *S100a8* and *S100a9* mRNA and S100a8 protein is markedly upregulated in WT STZ-HFD but not in *Tlr4* KO STZ-HFD mice, and S100a8 is predominantly expressed by glomerular macrophages in WT STZ-HFD mice. (a) Gene expression of *Tlr4*, *S100a8* and *S100a9* in glomeruli determined by real-time RT-PCR. White bars, WT; black bars, KO. Data are means±SEM. n=4-11. *p<0.05, **p<0.01. $^{\$}p$<0.05, $^{\$\$}p$<0.01 for similarly treated KO vs. WT. (b) Glomerular S100a8 protein expression (brown) examined by immunohistochemistry. Magnification, 40x. (c) Localization Mac-2 (brown in Fig. 4c-1, pseudocolored with green in 4c-3, by immunohisochemistry), S100a8 (red in 4c-2 and 4c-3, by immunofluorescence) and their overlaps (yellow in 4c-3) in glomeruli of WT STZ-HFD mice.

Fig. 5

Expression of S100A8 (brown) is observed in glomeruli of patients with diabetic nephropathy by immunohistochemistry. (a) Minor glomerular abnormality. (b) Minimal change nephrotic syndrome. (c) Mild and (d) severe cases of diabetic nephropathy.

Fig. 6

S100a8 expression in bone marrow-derived macrophages (BMDM) is synergistically induced by high glucose and palmitate in a Tlr4-dependent manner. (a, b) *S100a8* mRNA expression by real-time RT-PCR in BMDM from WT (a) and *Tlr4* KO (b) mice cultured under low or high (100 or 450 mg/dl) glucose conditions, and effects of palmitate (10-200 μM). Data are means±SEM. n=6. (c) *Tlr4* mRNA expression in WT BMDM. n=6. Open bars, WT low glucose; Solid bars, KO low glucose; chequered bars, high glucose conditions. *p< 0.05, **p< 0.01.

Fig. 7

Exacerbation of STZ-induced diabetic nephropathy by HFD is associated with increased phosphorylation of proteins involved in Trif-dependent and common pathways of Tlr4 signaling cascade in WT kidney but not in *Tlr4* KO kidney. (a) Schema describing known Tlr4 signaling cascade. Common pathway can be activated both through Myd88-dependent and Trif-dependent pathways. Key molecules analyzed in b are highlighted as elliptical objects. (b, c) Western blot analyses of Tlr4 signaling and quantitative evaluation. White bars, WT; black bars, KO. Data are means±SEM. n=4. *p<0.05, **p<0.01. $^{\$\$}p$<0.01 for similarly treated KO vs. WT.

Electronic supplementary material

ESM Table 1

Primer and probe sequences for real-time RT-PCR

ESM Table 2

List of primary antibodies used in this study

ESM Table 3

Pro-nflammatory and extracellular matrix-associated gene expression in whole kidney and glomeruli of WT mice treated with STZ and/or HFD by real-time RT-PCR.

ESM Table 4

Gene expression profiles of glomeruli and whole kidney in two different types of diabetic mice by microarray

ESM Table 5

PCR Array analysis of genes involved in TLR-downstream signaling cascade in kidneys of WT and *Tlr4* KO mice treated with STZ and/or HFD

ESM Fig. 1

Treatment of *db/db* mice with HFD exacerbates albuminuria.

ESM Fig. 2

Renal interstitial macrophage infiltration is markedly enhanced in WT mice co-treated with STZ and HFD, but not in *Tlr4* KO mice.

ESM Fig. 3

Gene expression levels of *Tlr4* and *S100a8* are elevated in glomeruli of two different types of diabetic mice by real-time RT-PCR.

ESM Fig. 4

Interstitial expression of *Tlr4*, *S100a8* and *S100a9* mRNA is not altered in WT and *Tlr4* KO mice co-treated with STZ and HFD.

ESM Fig. 5

Co-treatment by STZ and HFD causes markedly increased number of S100a8-positive cells in WT but not in *Tlr4* KO glomeruli.

ESM Fig. 6

Gene expression levels of *Cd36* and *Srebp1c* in the kidney and *S100a8* in the liver and aorta by real-time RT-PCR in mice treated with STZ and/or HFD.

Figure 1

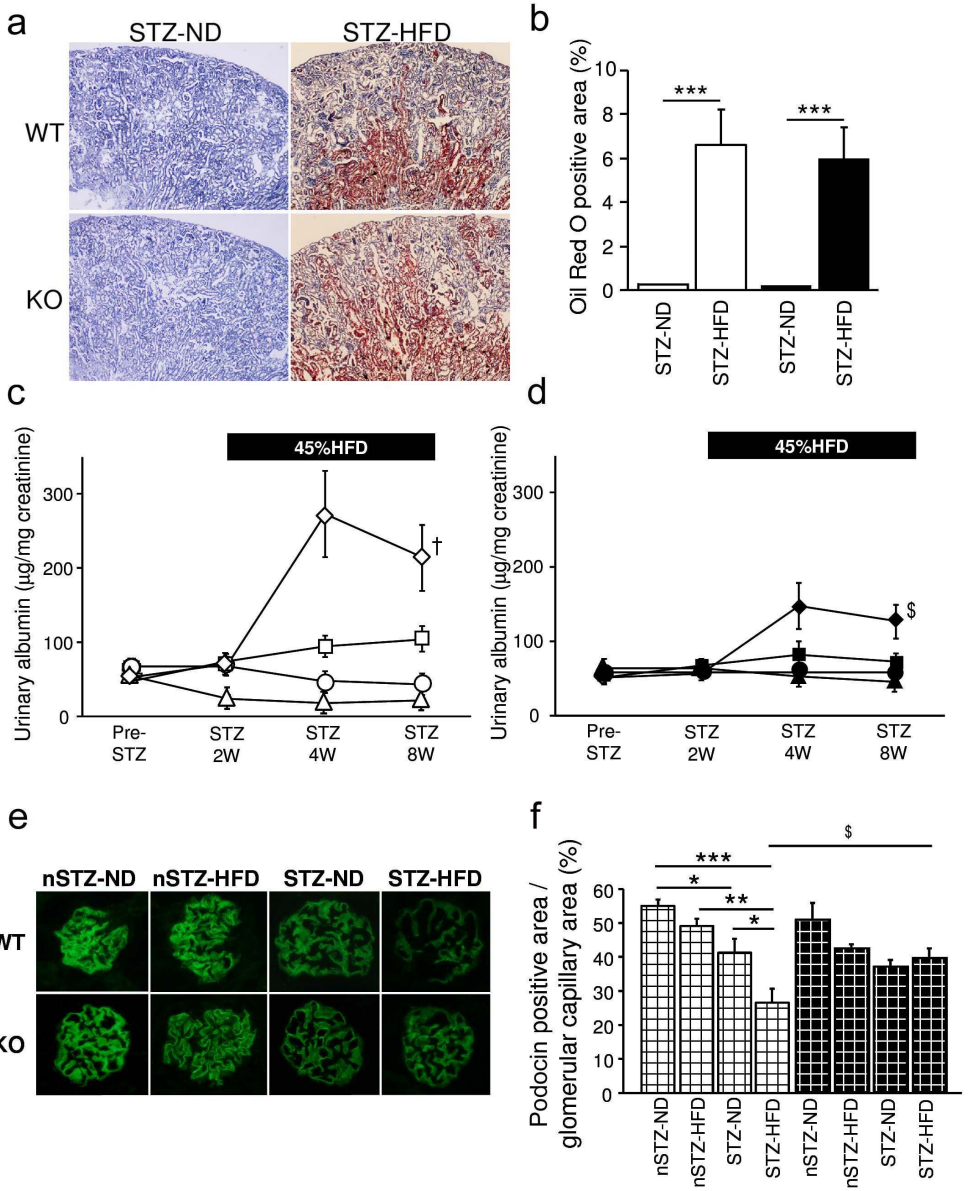
a
STZ-ND
STZ-HFD
WT
KO
b
Oil Red O positive area (%)
10
8
6
4
2
0
***
***
STZ-ND
STZ-HFD
STZ-ND
STZ-HFD
c
45%HFD
Urinary albumin (μg/mg creatinine)
300
200
100
0
†
Pre-STZ
STZ 2W
STZ 4W
STZ 8W
d
45%HFD
Urinary albumin (μg/mg creatinine)
300
200
100
0
$
Pre-STZ
STZ 2W
STZ 4W
STZ 8W
e
nSTZ-ND
nSTZ-HFD
STZ-ND
STZ-HFD
WT
KO
f
Podocin positive area / glomerular capillary area (%)
60
50
40
30
20
10
0
***
*
**
*
$
nSTZ-ND
nSTZ-HFD
STZ-ND
STZ-HFD
nSTZ-ND
nSTZ-HFD
STZ-ND
STZ-HFD

Figure 2

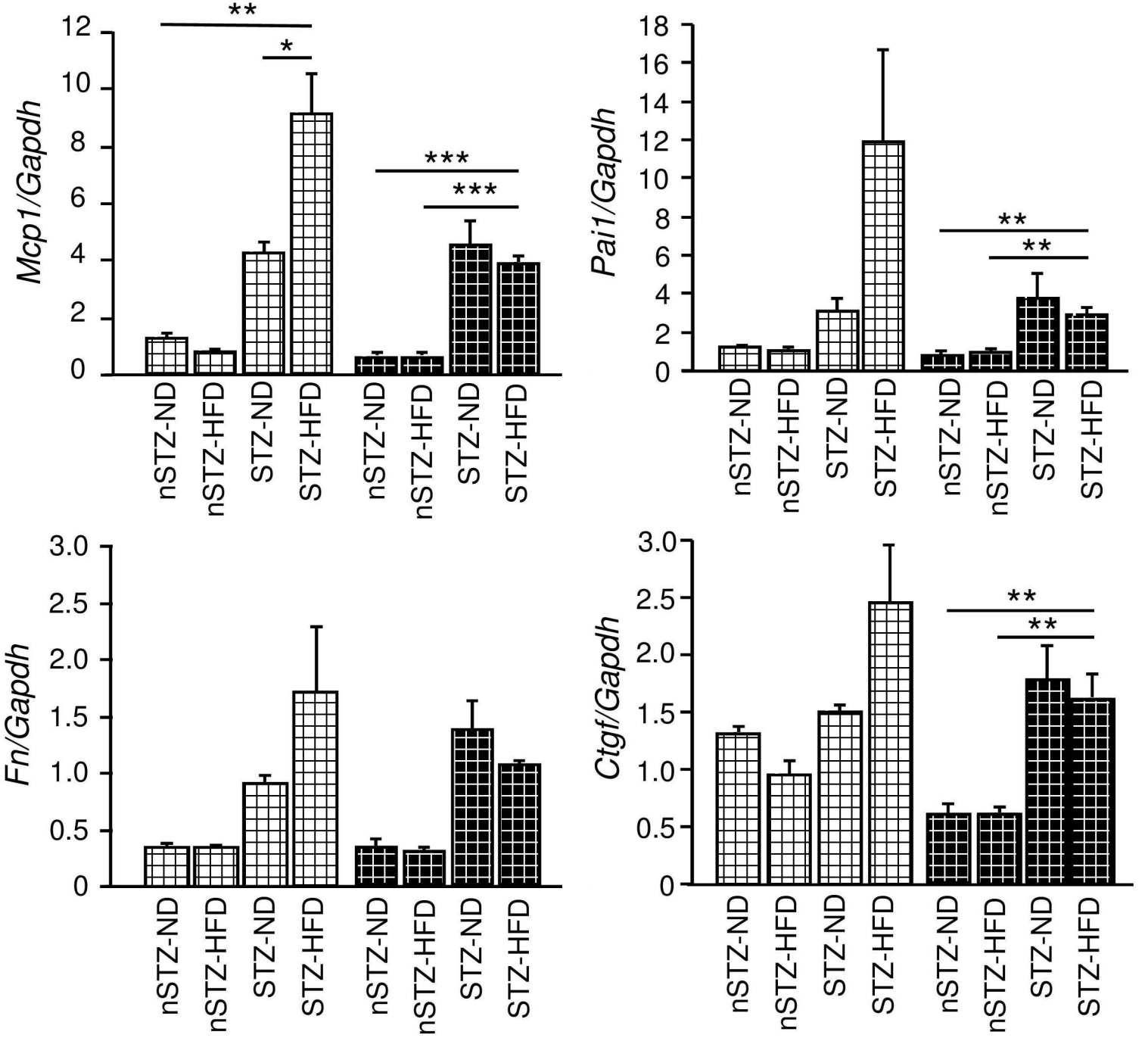
Mcp1/Gapdh
Pai1/Gapdh
Fn/Gapdh
Ctgf/Gapdh
nSTZ-ND
nSTZ-HFD
STZ-ND
STZ-HFD
*
**
***

Figure 3

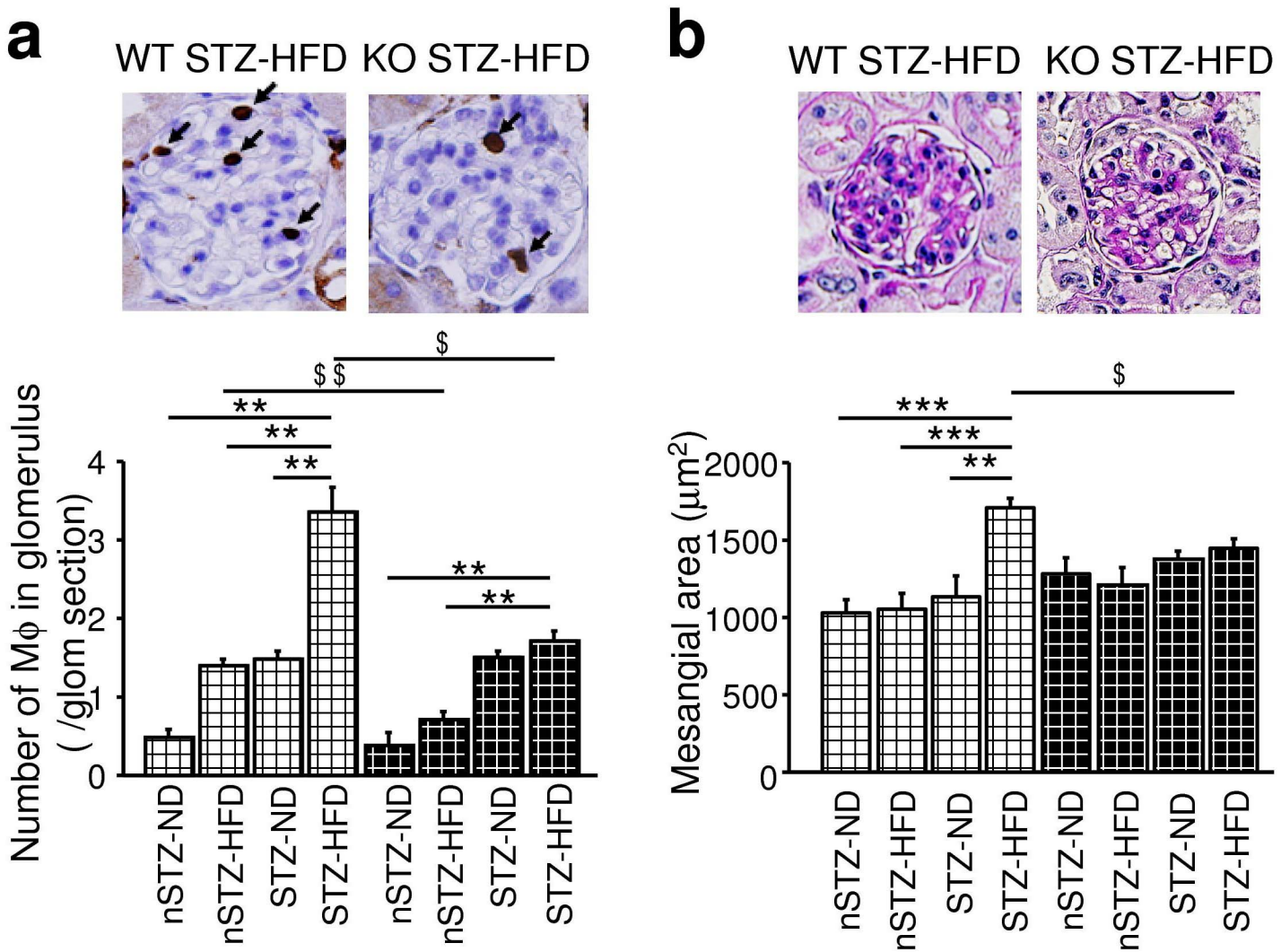
a
WT STZ-HFD
KO STZ-HFD
Number of Mϕ in glomerulus
(/glom section)
0
1
2
3
4
**
**
**
**
**
$
$
$
nSTZ-ND
nSTZ-HFD
STZ-ND
STZ-HFD
nSTZ-ND
nSTZ-HFD
STZ-ND
STZ-HFD
b
WT STZ-HFD
KO STZ-HFD
Mesangial area (μm2)
0
500
1000
1500
2000
***
***
**
$
nSTZ-ND
nSTZ-HFD
STZ-ND
STZ-HFD
nSTZ-ND
nSTZ-HFD
STZ-ND
STZ-HFD

Figure 4

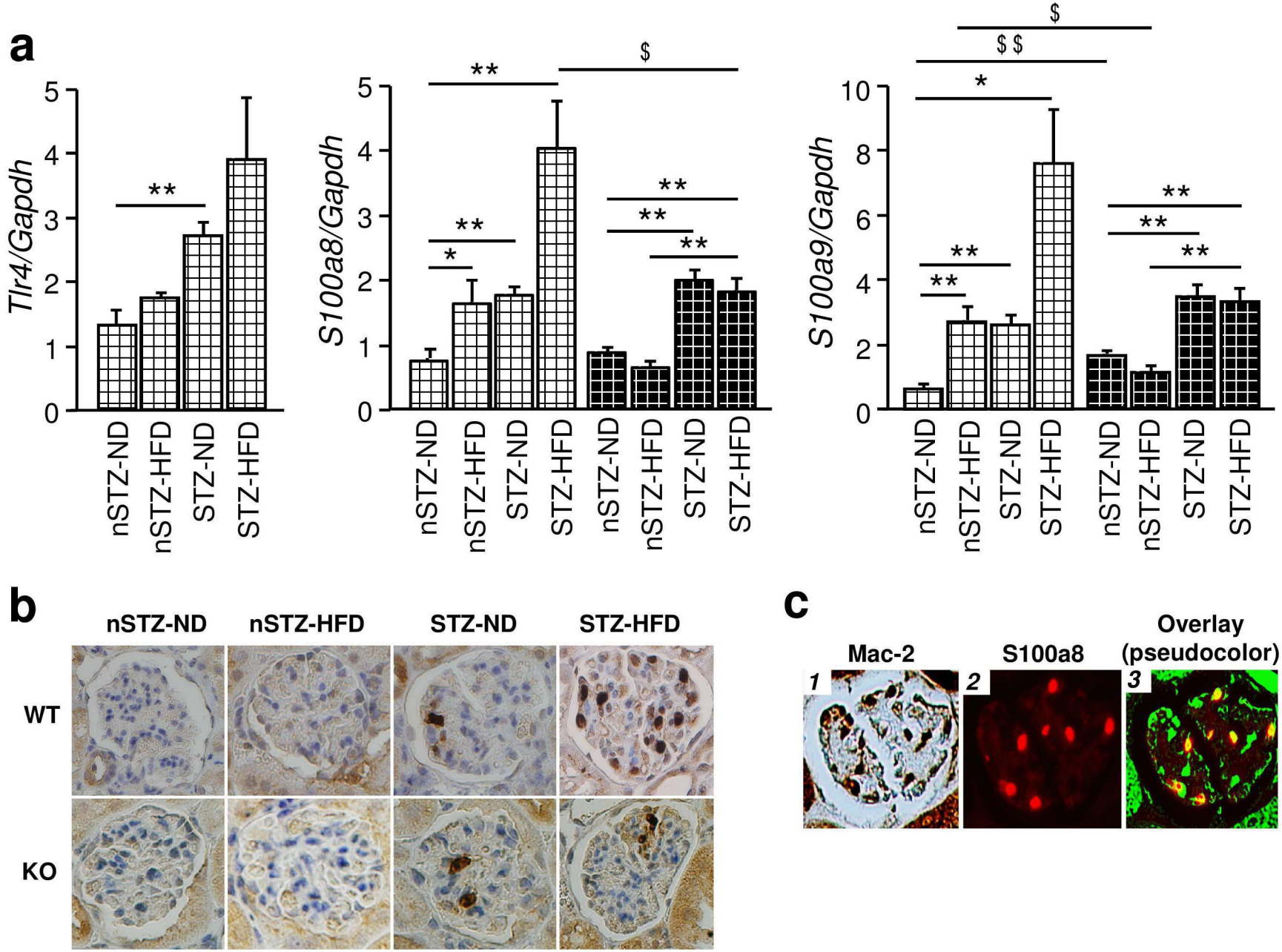
a
Tlr4/Gapdh
S100a8/Gapdh
S100a9/Gapdh
nSTZ-ND
nSTZ-HFD
STZ-ND
STZ-HFD
b
WT
KO
c
Mac-2
S100a8
Overlay (pseudocolor)
1
2
3

Figure 5

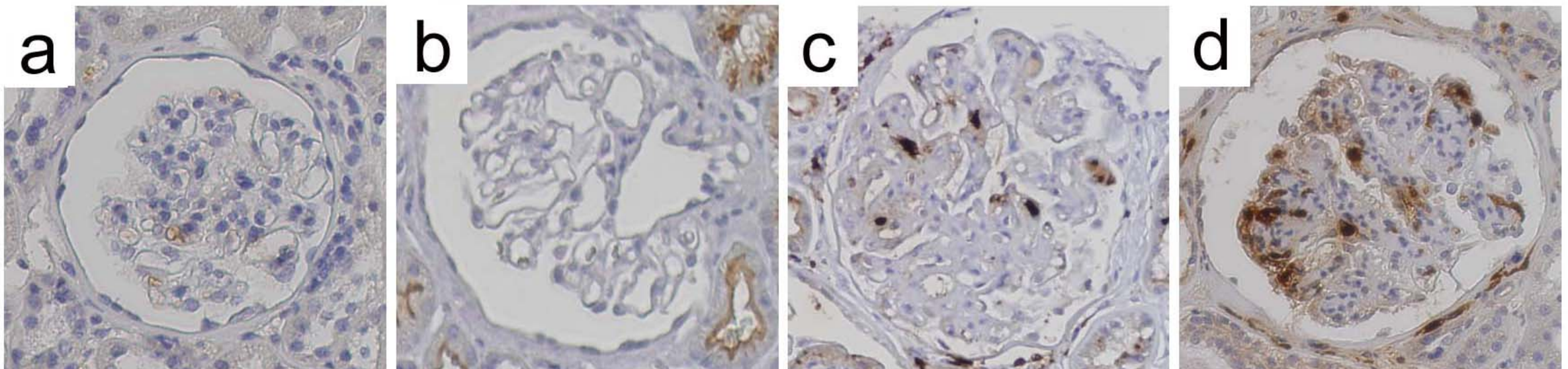

Figure 6

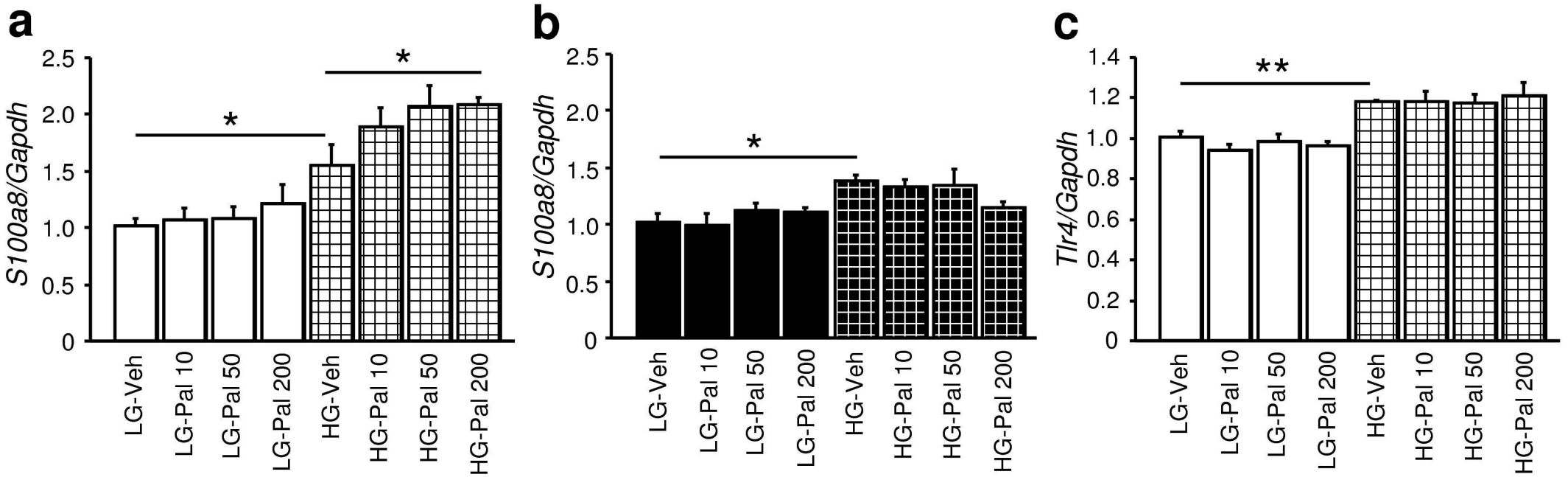
a
S100a8/Gapdh
2.5
2.0
1.5
1.0
0.5
0
*
*
LG-Veh
LG-Pal 10
LG-Pal 50
LG-Pal 200
HG-Veh
HG-Pal 10
HG-Pal 50
HG-Pal 200
b
S100a8/Gapdh
2.5
2.0
1.5
1.0
0.5
0
*
LG-Veh
LG-Pal 10
LG-Pal 50
LG-Pal 200
HG-Veh
HG-Pal 10
HG-Pal 50
HG-Pal 200
c
Tlr4/Gapdh
1.4
1.2
1.0
0.8
0.6
0.4
0.2
0
**
LG-Veh
LG-Pal 10
LG-Pal 50
LG-Pal 200
HG-Veh
HG-Pal 10
HG-Pal 50
HG-Pal 200

Figure 7

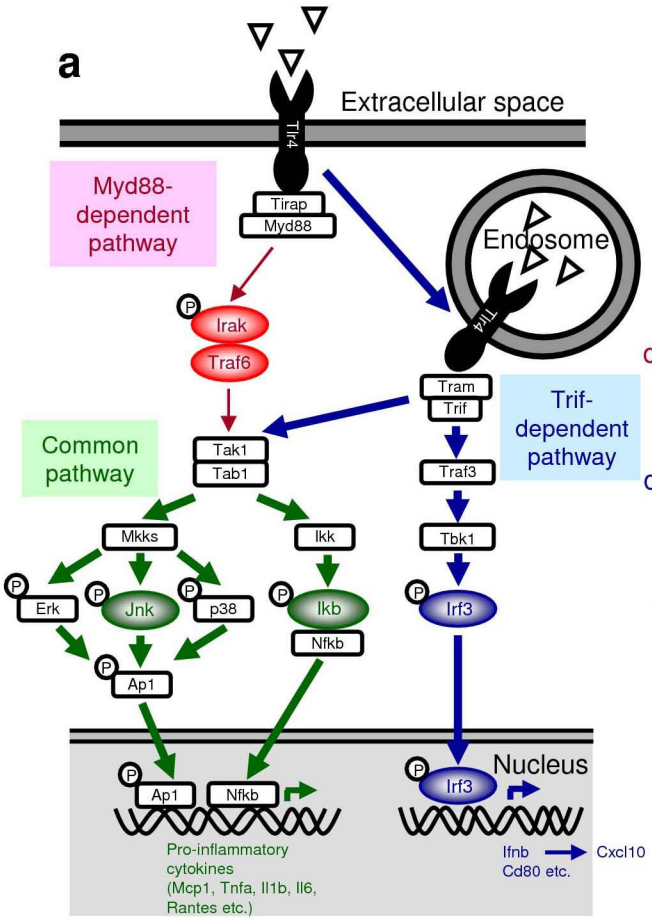
a
Extracellular space
Tlr4
Myd88-dependent pathway
Tirap
Myd88
Endosome
Tlr4
Irak
Traf6
Tram
Trif
Trif-dependent pathway
Common pathway
Tak1
Tab1
Traf3
Mkks
Ikk
Tbk1
Erk
Jnk
p38
Ikb
Irf3
Nfkb
Ap1
Nucleus
Ap1
Nfkb
Irf3
Pro-inflammatory cytokines (Mcp1, Tnfa, Il1b, Il6, Rantes etc.)
Ifnb
Cxcl10
Cd80 etc.

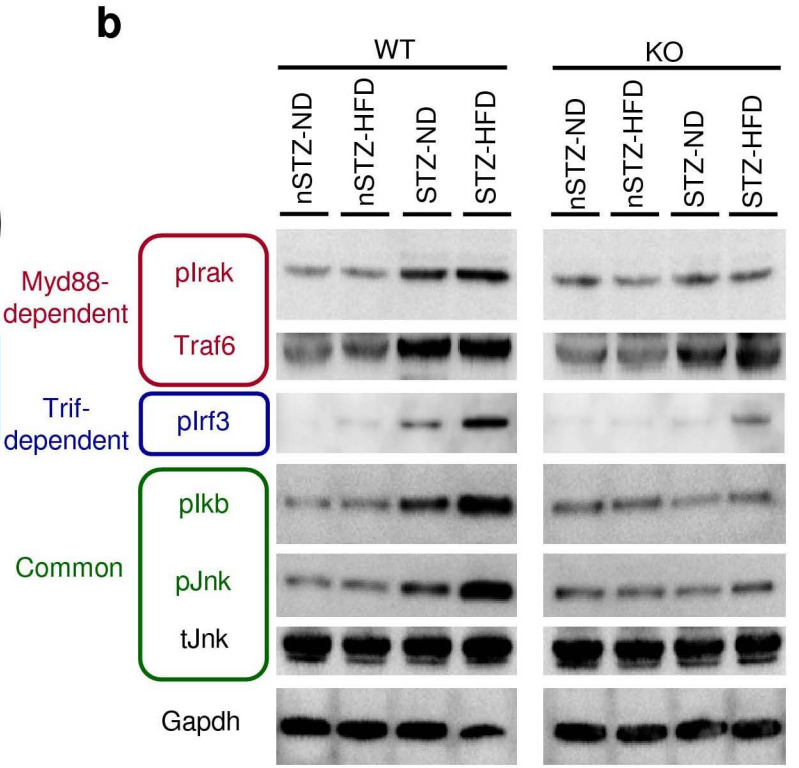
b
WT
KO
nSTZ-ND
nSTZ-HFD
STZ-ND
STZ-HFD
Myd88-dependent
pIrak
Traf6
Trif-dependent
pIrf3
Common
pIkb
pJnk
tJnk
Gapdh

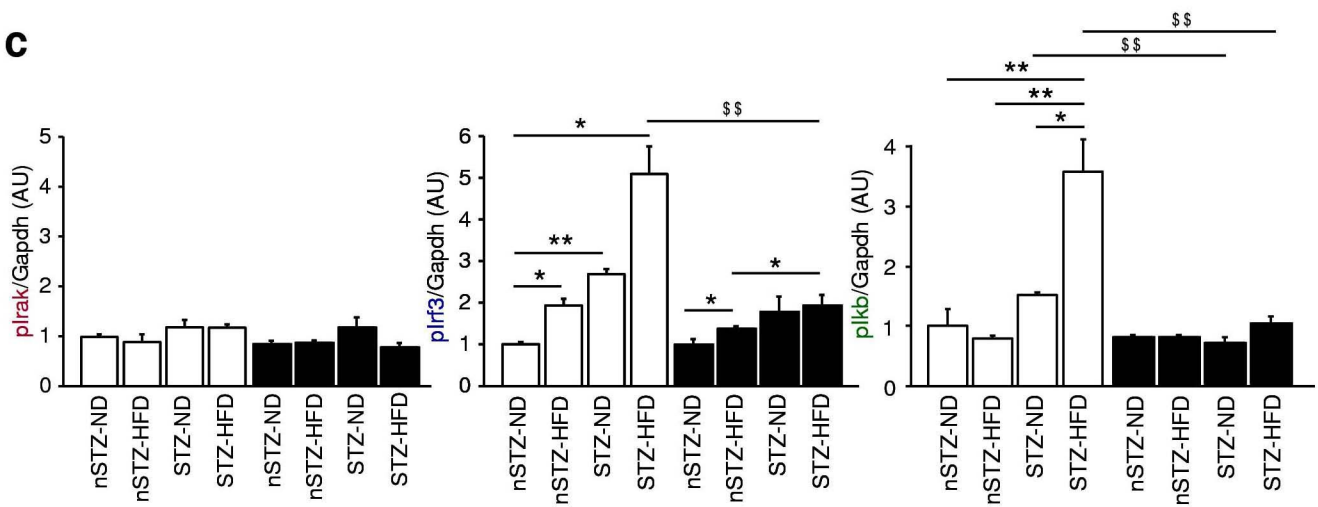
c
pIrak/Gapdh (AU)
pIrf3/Gapdh (AU)
pIkb/Gapdh (AU)
nSTZ-ND
nSTZ-HFD
STZ-ND
STZ-HFD
$$
**
*

ESM Table 1

Primer and probe sequences for real-time RT-PCR

Gene	Forward primer	Reverse primer	Probe
Desmin	5'-AGAGCAGGATCAACCTTC-3'	5'-CTGACAACCTCTCCATCC-3'	5'-FAM-CCTTCTCTGCTCTCAACTTCCG-TAMRA-3'
Mcp1	5'-TTGGCTCAGCCAGATGCA-3'	5'-CCAGCCTACTCATTGGGATCA-3'	5'-FAM-CCCCACTCACCTGCTACTCATTCA-TAMRA-3'
F4/80	5'-TGGTGGTCATAATCTCTGCTTCTG-3'	5'-AGACAGGCCCCAGGAAACTC-3'	5'-FAM-CCCGTCTCTGTATTCAACCAGCAGCGATT-TAMRA-3'
Cd68	5'-GCGGTGGAATACAATGTGTCC-3'	5'-TTGGCCCAAGGGAGCTTG-3'	5'-FAM-CGCCATGAATGTCCACTGTGCTGCCT-TAMRA-3'
Tnfa	5'-AAGGCTGCCCCGACTACG-3'	5'-AGGTTGACTTTCTCCTGGTATGAG-3'	5'-FAM-AGGTTGACTTTCTCCTGGTATGAG-TAMRA-3'
Pai1	5'-AAGGTCAGGATCGAGGTAAACG-3'	5'-GCCGAACCACAAAGAAAGG-3'	5'-FAM-GAGCGGCACAGTGGCGTCTTCCTCC-TAMRA-3'
Tgfb1	5'-GACGTCACTGGAGTTGTACGG-3'	5'-GCTGAATCGAAAGCCCTGT-3'	5'-FAM-AGTGGCTGAACCAAGGAGACGGAA-TAMRA-3'
Fn	5'-ATCATTTCATGCCAAGTT-3'	5'-TCGCACTGGTAGAAGTTCCA-3'	5'-FAM-CCGACGAAGAGCCCTTACAGTTCCA-TAMRA-3'
COL4a3	5'-TGTGGATGCACGGTGTGTT-3'	5'-GTTCTCTTCACGGTGTGCTTGA-3'	5'-FAM-CCTTCCATCTCCTCCCTGACACCTTAGACT-TAMRA-3'
Ctgf	5'-TTCCCGAGAAGGGTCAAGCT-3'	5'-TCCTTGGGCTCGTCACACA-3'	5'-FAM-CCTGGGAAATGCTGCAAGGAGTGG-TAMRA-3'
Mmp2	5'-CCTGGTTTCACCCTTTCTGCT-3'	5'-CGAGCGAAGGGCATACAAA-3'	5'-FAM-CCCAGATACCTGCACCACCTTAACTGTTGC-TAMRA-3'
Tlr4	5'-CTTCAGTGGCTGGATTTATC-3'	5'-GAGGTGGTGTAAGCCATG-3'	5'-FAM-CATGCCTTGTCTTCAATTGTTTCAA-TAMRA-3'
S100a8	5'-ATCCTTTGTCAGCTCCGTCTTC-3'	5'-GGGCATGGTGATTTCCTTGTATATT-3'	5'-FAM-ATCTTTCGTGACAATGCCGTCTGAACTGGA-TAMRA-3'
S100a9	5'-GAAGGAAGGACACCCTGACAC-3'	5'-TTTATGAGGGCTTCATTTCTCTTCTC-3'	5'-FAM-AAGGTTGCCAACTGTGCTTCCACCATT-TAMRA-3'
Hmgb1	5'-GGACCCCAATGCACCCAAG-3'	5'-TCACCAATGGATAAGCCAGGATG-3'	5'-FAM-CCTCCTTCGGCCTTCTTCTTGTTCTGTTCT-TAMRA-3'

Primer and probe sets for *Il1b* (*IL-1β*) and *Gapdh* were purchased from Applied Biosystems.

ESM Table 2

List of primary antibodies used in this study

Antibody Species	Antigen	Company	Method	Corresponding Data
rabbit	mouse Podocin	Sigma-Aldrich, St Louis, MO, USA	IF	Fig. 1e, f
goat	mouse S100a8	R&D systems, Minneapolis, MN, USA	IHC	Fig. 4b, c
rat monoclonal	mouse Mac-2	Cedarlane, Burlington, Ontario, Canada	IHC	Fig. 4c
mouse monoclonal	human S100A8	BMA Biomedicals, Rheinstrasse, Switzerland	IHC	Fig. 5
mouse monoclonal	mouse pIkb	Cell Signaling, Boston, MA, USA	WB	Fig. 7b, c
mouse monoclonal	mouse pJnk	Santa Cruz Biotechnology, Santa Cruz, CA, USA	WB	Fig. 7b
rabbit	mouse tJnk	Santa Cruz Biotechnology, Santa Cruz, CA, USA	WB	Fig. 7b
rabbit	mouse pIrak	Abcam, Cambridge, CA, UK	WB	Fig. 7b, c
rabbit	mouse Traf6	MBL, Nagoya, Japan	WB	Fig. 7b
rabbit	mouse pIrf3	Cell Signaling, Boston, MA,USA	WB	Fig. 7b, c
mouse monoclonal	mouse Gapdh	Santa Cruz Biotechnology, Santa Cruz, CA, USA	WB	Fig. 7b, c

IHC, immunohistochemistry; IF, immunofluorescence; WB, Western blot.

ESM Table 3

Pro-inflammatory and extracellular matrix (ECM)-associated gene expression in whole kidney and glomeruli of WT mice treated with STZ and/or HFD by real-time RT-PCR.

Gene name	Whole kidney				Glomerulus			
	WT nSTZ-ND	WT nSTZ-HFD	WT STZ-ND	WT STZ-HFD	WT nSTZ-ND	WT nSTZ-HFD	WT STZ-ND	WT STZ-HFD
Pro-inflammatory gene								
Mcp1	1.0±0.1	1.1±0.1	7.6±1.3*	14.1±2.0**##†	1.1±0.2	0.6±0.1	4.1±0.4***	9.0±1.4**#†
F4/80	1.0±0.2	1.2±0.1	1.6±0.4	3.8±0.6*#†	0.3±0.1	0.2±0.1	0.6±0.1*	1.0±0.2*#
Cd68	1.0±0.1	1.1±0.0	1.8±0.3	3.6±0.6*#†	0.4±0.1	0.4±0.1	0.8±0.1**	1.5±0.3*
Tnfa	1.0±0.3	1.0±0.2	1.9±0.5	2.4±0.3*#	0.6±0.1	0.5±0.1	1.4±0.1**	1.7±0.4
Pai1	1.0±0.1	0.8±0.1	2.6±0.8	6.5±1.6#	1.1±0.1	0.9±0.2	3.0±0.7*	11.8±4.8
Il1b	1.0±0.2	1.4±0.2	0.7±0.2	1.5±0.2†	0.5±0.1	1.3±0.1**	1.1±0.2*	2.1±0.7
ECM-associated gene								
Tgfb1	1.0±0.0	1.1±0.0	1.2±0.1	1.6±0.1*†	0.9±0.1	0.9±0.1	1.6±0.1***	2.4±0.3*
Fn	1.0±0.6	0.9±0.1	1.7±0.3	2.7±0.5*#	0.3±0.0	0.3±0.0	0.9±0.1***	1.7±0.6
Col4a3	1.0±0.0	1.2±0.0**	0.6±0.1**	0.9±0.1##†	1.5±0.1	1.6±0.1	1.8±0.1	2.4±0.4
Ctgf	1.0±0.1	0.8±0.1	0.9±0.0	1.0±0.2	1.3±0.1	0.9±0.1*	1.5±0.1	2.4±0.5
Mmp2	1.0±0.1	1.1±0.1	2.9±0.3**	5.6±1.1*#	1.0±0.2	1.0±0.2	2.6±0.2**	6.9±2.1

The gene expression levels divided by *Gapdh* expression levels in respective groups were normalized to the mean levels in wild-type, control whole kidneys (WT nSTZ-ND group), and expressed in arbitrary units. Data are means±SEM. n=4-11. *p<0.05 vs. nSTZ-ND, $^{\#}p$< 0.05 vs. nSTZ-HFD, $^{\dagger}p$< 0.05 vs. STZ-ND. Two symbols, p<0.01; three symbols, p<0.001.

ESM Table 4

Gene expression profiles of glomeruli and whole kidney in two different types of diabetic mice by microarray

Gene Title	*Gene Symbol*	Wk	Glomerulus					Glomerulus	
		Control B6 wk	Control non-STZ	STZ	Control FVB/N	A-ZIP	B6 Glom/Wk ratio	STZ/non-STZ ratio	A-ZIP/FVB-N ratio
Toll-like receptors									
toll-like receptor 4	*Tlr4*	12.2	30.1	51.9	13.2	76.3	2.5	1.7	5.8
toll-like receptor 1	*Tlr1*	17.4	9.3	0.5	5.8	13.9	0.5	0.1	2.4
toll-like receptor 2	*Tlr2*	18.6	18.5	19.0	6.9	39.3	1.0	1.0	5.7
toll-like receptor 3	*Tlr3*	66.1	39.7	49.9	60.0	51.5	0.6	1.3	0.9
toll-like receptor 5	*Tlr5*	2.2	7.1	19.2	15.3	21.0	3.2	2.7	1.4
toll-like receptor 6	*Tlr6*	4.4	8.3	7.6	16.8	13.5	1.9	0.9	0.8
toll-like receptor 7	*Tlr7*	4.4	3.3	1.1	1.9	1.9	0.8	0.3	1.0
toll-like receptor 8	*Tlr8*	2.0	2.3	7.6	13.9	1.6	1.2	3.3	0.1
toll-like receptor 9	*Tlr9*	16.2	17.9	20.0	8.1	17.3	1.1	1.1	2.1
toll-like receptor 12	*Tlr12*	17.7	15.9	15.1	11.1	20.3	0.9	0.9	1.8
toll-like receptor 13	*Tlr13*	15.6	2.6	16.2	3.9	10.3	0.2	6.2	2.6
Endogenous ligands of TLR4									
myeloid-related protein 8	*S100a8*	10.5	31.2	73.2	13.1	43.2	3.0	2.3	3.3
myeloid-related protein 14	*S100a9*	11.5	27.7	66.5	7.0	52.1	2.4	2.4	7.4
serum amyloid A 3	*Saa3*	14.6	6.5	20.5	16.9	11.0	0.4	3.2	0.7
high mobility group box 1	*Hmgb1*	992.9	903.4	831.4	1375.7	1301.4	0.9	0.9	0.9
biglycan	*Bgn*	972.7	366.9	484.2	215.2	461.1	0.4	1.3	2.1
heat shock protein 1A (HSP70)	*Hspa1a*	184.6	125.8	84.2	395.9	1612.1	0.7	0.7	4.1
heat shock protein 1 (chaperonin 10, HSP60)	*Hspe1*	409.3	449.3	303.8	343.5	474.8	1.1	0.7	1.4
heat shock protein 90kDa alpha (cytosolic), class B member 1	*Hsp90ab1*	2090.3	2252.6	1534.1	2395.6	2928.7	1.1	0.7	1.2
hyaluronan synthase 2	*Has2*	4.2	8.2	3.0	1.1	5.6	2.0	0.4	5.1
hyaluronan synthase 3	*Has3*	9.7	0.6	0.8	1.3	0.8	0.1	1.3	0.6
hyaluronan synthase1	*Has1*	14.7	2.1	21.2	11.5	4.4	0.1	10.1	0.4
perlecan	*Hspg2*	52.5	35.5	48.1	25.3	39.0	0.7	1.4	1.5
syndecan 2	*Sdc2*	254.0	451.3	181.1	959.7	726.2	1.8	0.4	0.8
defensin beta 2	*Defb2*	2.2	2.6	8.0	2.4	0.9	1.2	3.1	0.4
elastase 2	*Ela2*	6.7	11.6	16.4	1.9	3.3	1.7	1.4	1.7
ECM-associated genes									
Transforming growth factor, beta 1	*Tgfb1*	10.2	13.8	23.2	14.5	23.5	1.4	1.7	1.6
fibronectin 1	*Fn1*	232.8	87.5	117.5	91.9	135.7	0.4	1.3	1.5
procollagen, type IV, alpha 1	*Col4a1*	349.3	266.1	384.4	332.5	583.6	0.8	1.4	1.8
procollagen, type IV, alpha 3	*Col4a3*	550.5	409.1	904.2	193.2	560.7	0.7	2.2	2.9
procollagen, type I, alpha 1	*Col1a1*	152.0	15.5	49.0	23.2	15.3	0.1	3.2	0.7
connective tissue growth factor	*Ctgf*	928.4	788.0	1245.4	475.9	4427.1	0.8	1.6	9.3
matrix metalloproteinase 2	*Mmp2*	40.7	25.2	51.9	26.0	120.2	0.6	2.1	4.6
Pro-inflammatory genes									
chemokine (C-C motif) ligand 2	*Ccl2*	0.8	2.3	22.5	12.5	19.8	2.9	9.8	1.6
chemokine (C-C motif) receptor 2	*Ccr2*	20.4	17.0	39.2	10.5	16.3	0.8	2.3	1.6
EGF-like module containing, mucin-like, hormone receptor-like sequence 1	*Emr1*	72.8	40.5	47.4	16.7	21.1	0.6	1.2	1.3
CD68 antigen	*Cd68*	28.2	11.3	13.2	9.0	29.2	0.4	1.2	3.2
tumor necrosis factor	*Tnf*	0.9	2.3	8.9	2.3	11.5	2.6	3.9	5.0
interleukin 1 beta	*Il1b*	19.0	15.1	24.2	9.6	25.0	0.8	1.6	2.6
interleukin 6	*Il6*	6.2	2.2	6.0	0.2	6.2	0.4	2.7	31.0
chemokine (C-C motif) ligand 5 (RANTES)	*Ccl5*	15.8	7.0	3.8	1.3	4.8	0.4	0.5	3.7
chemokine (C-X-C motif) ligand 10	*Cxcl10*	15.4	40.1	76.3	31.4	34.7	2.6	1.9	1.1
advanced glycosylation end product-specific receptor	*Ager*	14.4	30.8	15.6	5.0	2.7	2.1	0.5	0.5

(Legend for ESM Table 4)

Gene expression levels in control non-STZ C57BL/6J whole kidney (control B6 wk) are shown as references. Relative expression levels of control non-STZ glomeruli vs. whole kidney (B6 Glom/Wk raio), STZ vs. non-STZ glomeruli (STZ/non-STZ raio) and A-ZIP/F-1 vs. FVB-N glomeruli (A-ZIP/FVB-N ratio) are also shown. Of note, the numbers indicate signal intensities of respective genes from microarray analysis, which cannot be used to compare different genes.

ESM Table 5

PCR Array analysis of genes involved in TLR-downstream signaling cascade in kidneys of WT and *Tlr4* KO mice treated with STZ and/or HFD

Data are expressed as fold changes from nSTZ-ND control.

Asterisk indicates efficient disruption of *Tlr4* gene expression.

Gene title	*Gene symbol*	Fold change from WT nSTZ-ND			
		WT STZ+ND	WT STZ+HFD	KO STZ+ND	KO STZ+HFD
Toll-like receptors					
Toll-like receptor 1	*Tlr1*	3.0	3.4	3.1	3.0
Toll-like receptor 2	*Tlr2*	2.4	5.8	6.7	5.4
Toll-like receptor 3	*Tlr3*	1.6	1.4	1.1	0.9
Toll-like receptor 4	*Tlr4*	2.9	5.1	0.0*	0.0*
Toll-like receptor 5	*Tlr5*	2.6	2.9	3.4	5.3
Toll-like receptor 6	*Tlr6*	4.3	3.7	2.8	2.2
Toll-like receptor 7	*Tlr7*	2.3	3.9	2.6	2.2
Toll-like receptor 8	*Tlr8*	2.7	7.5	4.3	3.0
Toll-like receptor 9	*Tlr9*	1.7	2.1	2.9	2.3
Mucin 13, epithelial transmembrane	*Muc13*	7.8	18.0	5.9	6.3
Adaptors and TLR interacting proteins					
Bruton agammaglobulinemia tyrosine kinase	*Btk*	2.4	3.1	2.4	1.8
CD14 antigen	*Cd14*	5.5	4.4	4.7	3.9
High mobility group box 1	*Hmgb1*	0.9	0.9	0.8	0.7
Harvey rat sarcoma virus oncogene 1	*Hras1*	0.7	0.7	1.4	1.4
Heat shock protein 1A	*Hspa1a*	1.1	0.5	0.5	0.4
Heat shock protein 1 (chaperonin)	*Hspd1*	0.6	0.8	0.6	0.7
Lymphocyte antigen 86 （MD-1)	*Ly86*	2.0	3.1	1.5	3.5
Lymphocyte antigen 96 (MD-2)	*Ly96*	1.5	1.4	1.1	1.0
Mitogen-activated protein kinase 8 interacting protein 3 (JIP3)	*Mapk8ip3*	1.0	1.0	1.3	1.2
Myeloid differentiation primary response gene 88	*Myd88*	2.9	2.0	1.1	0.9
Pellino 1	*Peli1*	1.3	1.5	1.0	0.8
Peptidoglycan recognition protein 1	*Pglyrp1*	8.1	4.8	2.3	2.1
Receptor (TNFRSF)-interacting serine-threonine kinase 2	*Ripk2*	1.7	1.8	1.3	1.2
Toll-like receptor adaptor molecule 1	*Ticam1*	0.7	0.4	0.8	0.7
Toll-like receptor adaptor molecule 2	*Ticam2*	3.1	4.8	8.7	5.7
Toll-interleukin 1 receptor (TIR) domain-containing adaptor protein	*Tirap*	1.3	1.4	1.5	1.2
Toll interacting protein	*Tollip*	0.8	0.7	0.9	0.8
Effectors					
Caspase 8	*Casp8*	1.5	1.2	0.9	0.9
Fas (TNFRSF6)-associated via death domain	*Fadd*	1.0	0.6	0.9	1.0
Interleukin-1 receptor-associated kinase 1	*Irak1*	1.4	1.1	1.0	1.0
Interleukin-1 receptor-associated kinase 2	*Irak2*	0.9	0.8	1.0	0.9
Mitogen-activated protein kinase kinase kinase 7	*Map3k7*	1.5	1.4	1.0	1.0
Nuclear receptor subfamily 2, group C, member 2 (TAK1)	*Nr2c2*	1.2	0.9	1.0	0.9
Peroxisome proliferator activated receptor alpha	*Ppara*	0.7	0.9	0.4	0.5
Eukaryotic translation initiation factor 2-alpha kinase 2	*Eif2ak2*	1.8	2.1	1.7	1.5
Tnf receptor-associated factor 6	*Traf6*	1.3	1.0	0.8	0.8
Ubiquitin-conjugating enzyme E2N	*Ube2n*	1.2	1.2	0.8	0.8
Ubiquitin-conjugating enzyme E2 variant 1	*Ube2v1*	0.9	0.8	1.1	1.2
Downstream pathways and target genes					
NFκB pathway					
Chemokine (C-C motif) ligand 2 (MCP-1)	*Ccl2*	9.6	24.8	11.5	8.0
Conserved helix-loop-helix ubiquitous kinase (IKKa)	*Chuk*	0.8	1.3	0.6	0.7
Colony stimulating factor 2 (granulocyte-macrophage) (GM-CSF)	*Csf2*	20.7	20.2	8.1	6.3
Colony stimulating factor 3 (granulocyte) (G-CSF)	*Csf3*	6.8	2.3	0.8	1.0
Interferon beta 1, fibroblast	*Ifnb1*	2.2	5.4	1.2	1.6
Interferon gamma	*Ifng*	3.2	2.4	1.7	1.9
Inhibitor of kappaB kinase beta (IKKb)	*Ikbkb*	1.0	1.0	0.8	0.9
Interleukin 1 alpha	*Il1a*	1.1	1.3	1.6	2.2
Interleukin 1 beta	*Il1b*	1.4	2.3	2.9	2.5
Interleukin 1 receptor, type I	*Il1r1*	2.6	1.9	1.8	1.4
Interleukin 2	*Il2*	13.4	27.7	2.3	2.2
Interleukin 6	*Il6*	4.8	6.4	8.9	7.7
Interleukin 10	*Il10*	79.0	47.6	4.4	3.8
Interleukin 12A	*Il12a*	1.1	1.6	2.7	4.0
Lymphotoxin A (TNFb)	*Lta*	2.3	1.1	2.3	2.8
Mitogen-activated protein kinase kinase kinase 1 (MEKK1)	*Map3k1*	1.4	1.3	1.2	1.0
Nuclear factor of kappa light polypeptide gene enhancer in B-cells 1, p105	*Nfkb1*	1.6	1.5	1.7	1.4
Nuclear factor of kappa light polypeptide gene enhancer in B-cells 2, p49/p100	*Nfkb2*	1.7	1.7	2.8	2.7
Nuclear factor of kappa light polypeptide gene enhancer in B-cells inhibitor, alpha	*Nfkbia*	2.5	3.5	1.1	1.5
Nuclear factor of kappa light polypeptide gene enhancer in B-cells inhibitor, beta	*Nfkbib*	3.3	2.3	1.5	1.5
Nuclear factor of kappa light polypeptide gene enhancer in B-cells inhibitor-like 1	*Nfkbil1*	1.9	1.4	0.9	0.9
Nuclear factor related to kappa B binding protein	*Nfrkb*	1.1	0.9	0.9	0.9
Reticuloendotheliosis oncogene	*Rel*	1.7	1.9	1.2	1.4
V-rel reticuloendotheliosis viral oncogene homolog A (avian)	*Rela*	1.3	1.2	1.5	1.3
Tumor necrosis factor (TNFa)	*Tnf*	9.3	4.3	3.6	2.9
Tumor necrosis factor, alpha-induced protein 3	*Tnfaip3*	2.3	3.3	2.5	2.5
Tumor necrosis factor receptor superfamily, member 1a	*Tnfrsf1a*	1.2	1.1	1.8	1.6
TNFRSF1A-associated via death domain	*Tradd*	1.0	1.0	1.2	1.2
JNK/p38 pathway					
ELK1, member of ETS oncogene family	*Elk1*	2.8	1.9	0.7	0.7
FBJ osteosarcoma oncogene	*Fos*	1.7	1.5	4.8	1.6
Jun oncogene	*Jun*	0.9	1.3	1.5	1.4
Mitogen-activated protein kinase kinase 3 (MKK3)	*Map2k3*	1.6	1.4	1.0	1.1
Mitogen-activated protein kinase kinase 4 (MKK4)	*Map2k4*	1.5	1.4	1.0	1.0
Mitogen-activated protein kinase kinase kinase 1 (MEKK1)	*Map3k1*	1.4	1.3	1.2	1.0
Mitogen-activated protein kinase 8 (JNK1)	*Mapk8*	1.2	1.1	0.5	0.6
Mitogen-activated protein kinase 9 (JNK2)	*Mapk9*	1.2	1.1	0.9	0.7
NF/IL6 pathway					
CCAAT/enhancer binding protein (C/EBP), beta	*Cebpb*	1.8	2.9	1.2	1.8
C-type lectin domain family 4, member e	*Clec4e*	1.4	3.0	2.0	2.3
Interleukin 6 receptor, alpha	*Il6ra*	1.3	1.3	1.9	1.4
Prostaglandin-endoperoxide synthase 2 (Cox-2)	*Ptgs2*	6.9	5.2	3.0	1.5
IRF pathway					
Chemokine (C-X-C motif) ligand 10 (IP-10)	*Cxcl10*	5.0	9.7	3.4	3.5
Interferon beta 1, fibroblast	*Ifnb1*	2.2	5.4	1.2	1.6
Interferon regulatory factor 1	*Irf1*	2.4	2.0	1.8	1.7
Interferon regulatory factor 3	*Irf3*	1.4	0.7	0.9	0.9
TANK-binding kinase 1	*Tbk1*	1.0	0.9	0.8	0.8
Regulation of adaptive immunity					
CD80 antigen	*Cd80*	9.9	17.6	6.5	5.9
CD86 antigen	*Cd86*	2.8	3.6	3.4	3.2
Receptor (TNFRSF)-interacting serine-threonine kinase 2	*Ripk2*	1.7	1.8	1.3	1.2
Tnf receptor-associated factor 6	*Traf6*	1.3	1.0	0.8	0.8

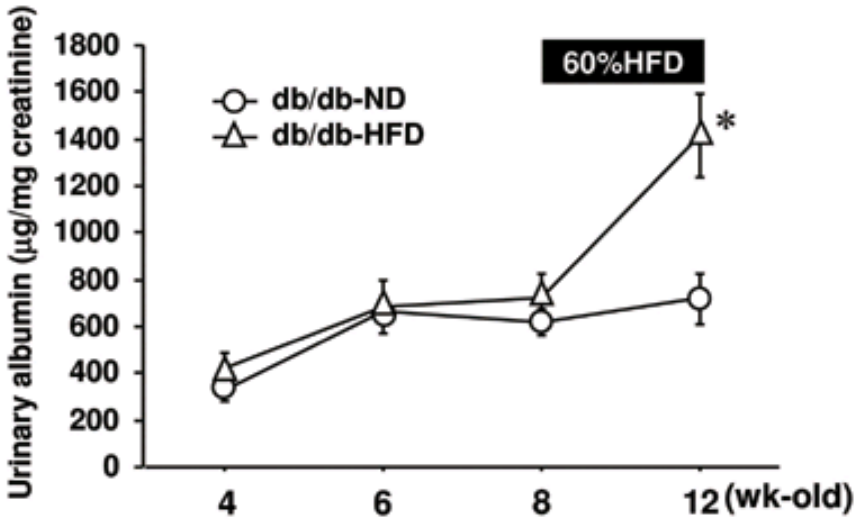

ESM Fig. 1

Treatment of *db/db* mice with high fat diet (HFD) exacerbates albuminuria. Data are means±SEM. n=5. *p< 0.05 vs. normal diet (ND).

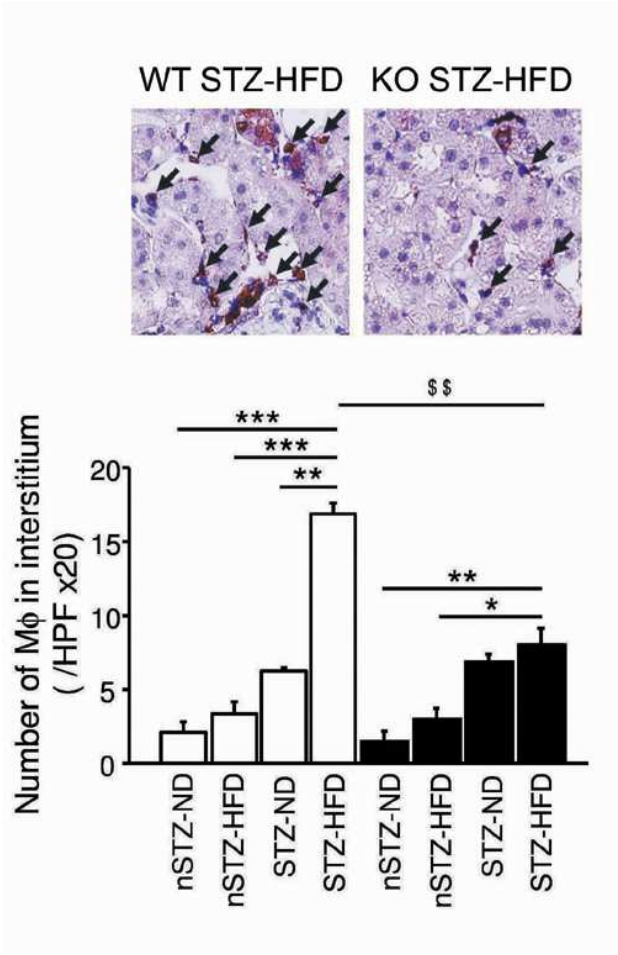

ESM Fig. 2

Renal interstitial macrophage infiltration is markedly enhanced in WT mice co-treated with STZ and HFD, but not in *Tlr4* KO mice. Interstitial macrophage number per 20 high power fields (HPF). Magnification, 20x. White bars, WT; black bars, KO. n=4-5. *p<0.05, **p<0.01. ***p<0.001. $^{\$\$}p$<0.01 for similarly treated KO vs. WT.

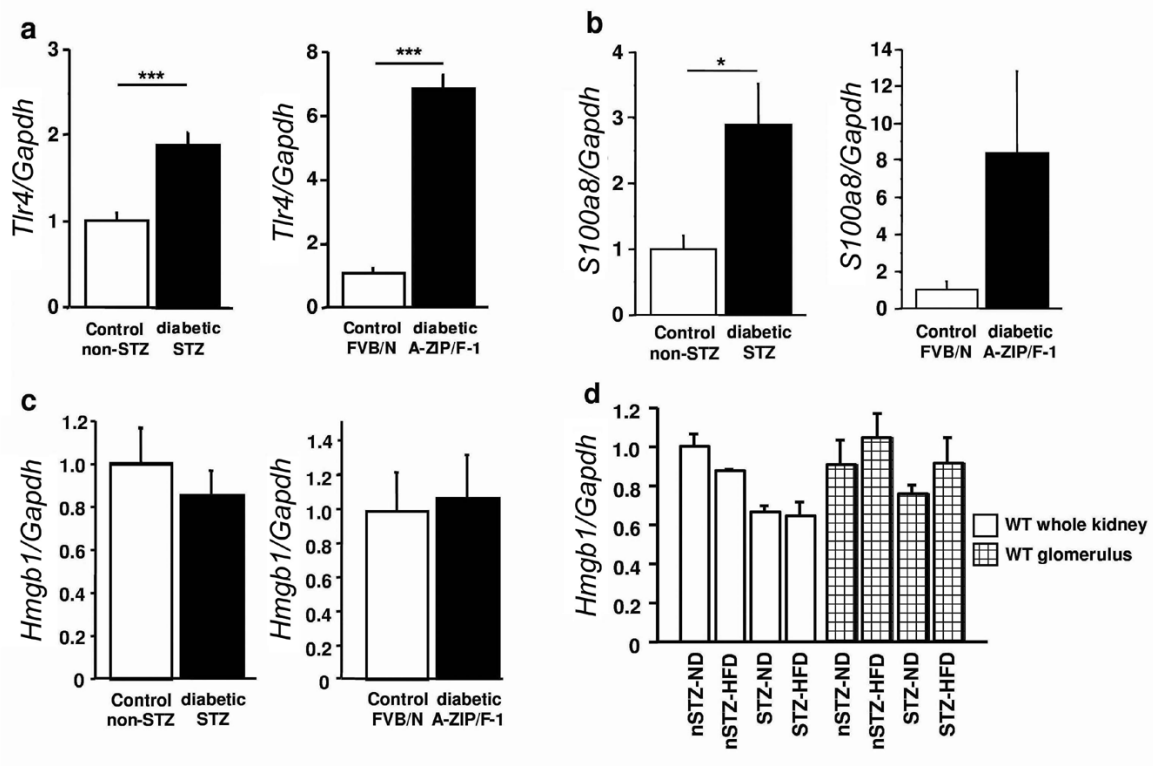

ESM Fig. 3

Gene expression levels of (a) *Tlr4* and (b) *S100a8* are elevated in glomeruli of two different types of diabetic mice by real-time RT-PCR. (c) Neither diabetes nor (d) HFD treatment causes upregulation of *Hmgb1* (encoding high mobility group box 1) expression in mouse glomeruli. Data are means±SEM. n=4-8. *p< 0.05, ***p< 0.001.

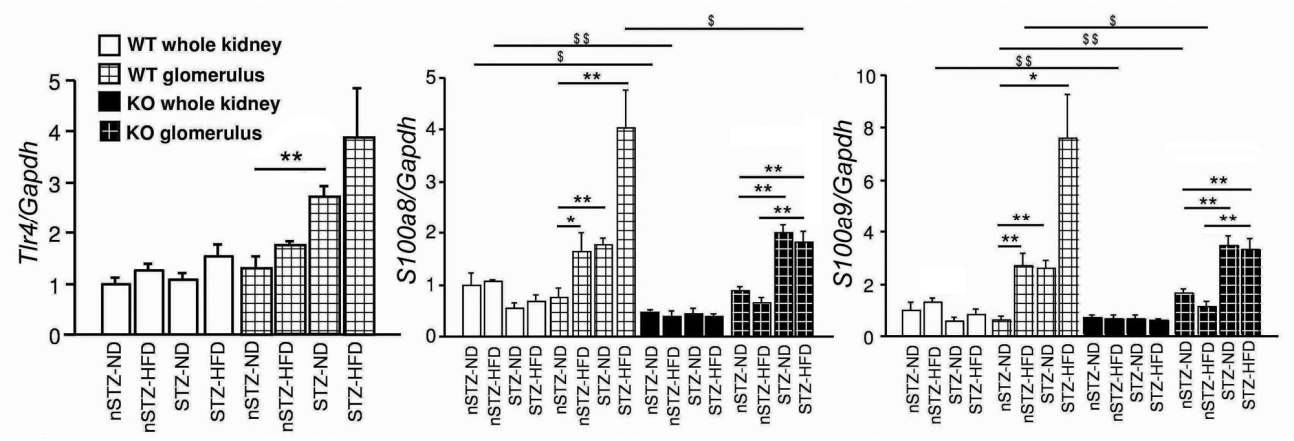

ESM Fig. 4

Interstitial expression of *Tlr4*, *S100a8* and *S100a9* mRNA is not altered in WT and *Tlr4* KO mice co-treated with STZ and HFD. Gene expressions of *Tlr4*, *S100a8* and *S100a9* in whole kidney and glomerulus determined by real-time RT-PCR are presented for comparison. Data are means±SEM. n=4-11. *p<0.05, **p<0.01. $^{\$}p$<0.05, $^{\$\$}p$<0.01 for similarly treated KO vs. WT.

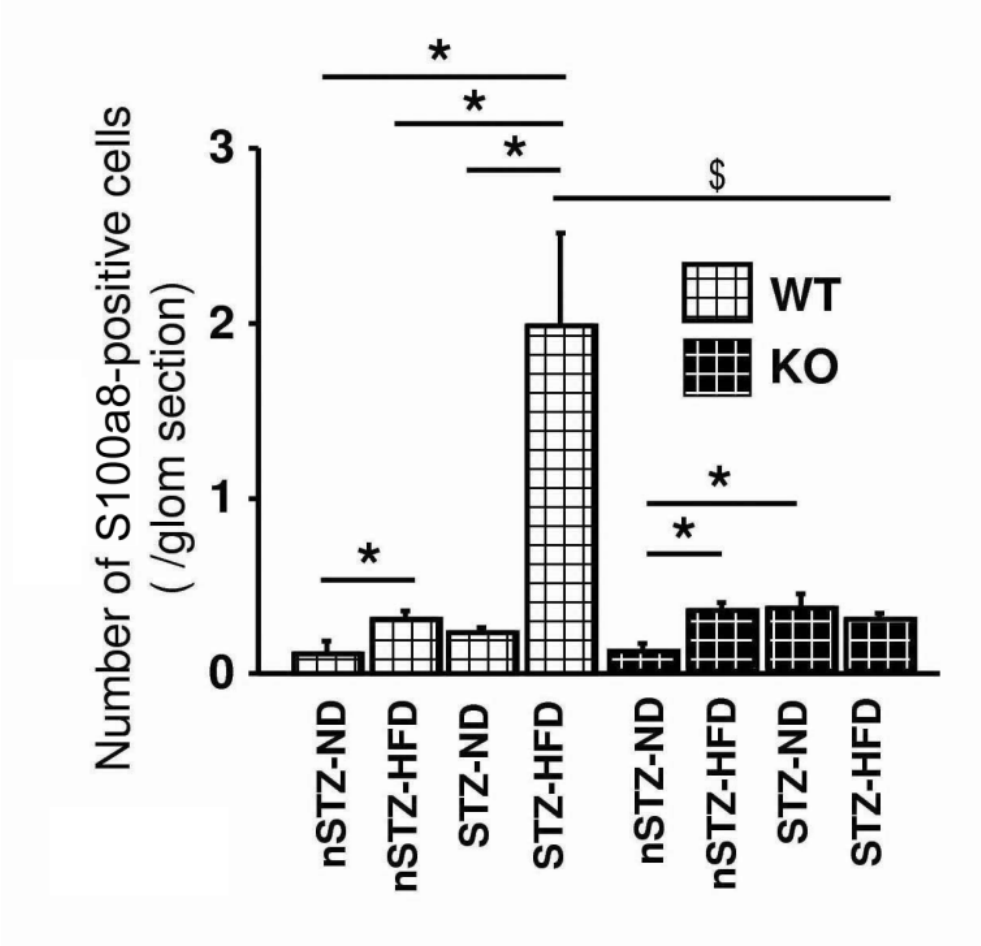

ESM Fig. 5

Co-treatment by STZ and HFD causes markedly increased number of S100a8-positive cells in WT but not in *Tlr4* KO glomeruli. Data are means±SEM. *n*=4-6. **p*< 0.05, $^{\$}$*p*< 0.05 for similarly treated KO vs. WT.

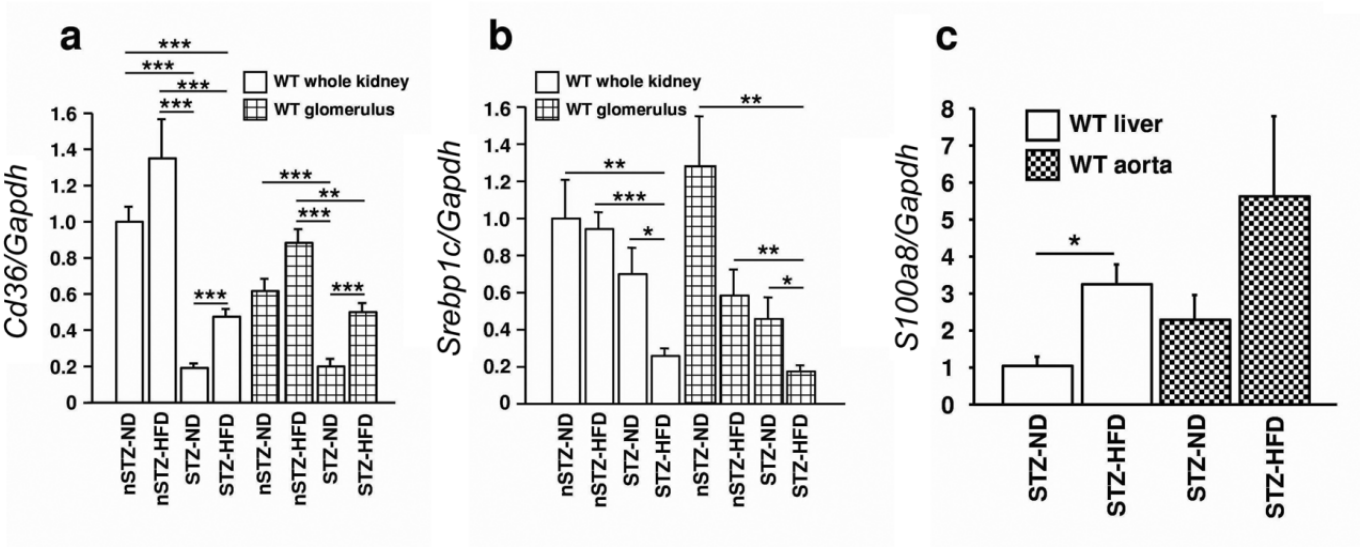

ESM Fig. 6

Gene expression levels of *Cd36* and *Srebp1c* in the kidney and *S100a8* in the liver and aorta by real-time RT-PCR in mice treated with STZ and/or HFD. Upregulation in (a) *Cd36* or (b) *Srebp1c* expression in glomeruli does not explain synergistic effects of STZ and HFD upon renal injury. Organs were collected at ad libitum feeding conditions. Data are means±SEM. *n*=4-11. (c) Treatment of STZ mice with HFD results in a tendency of increased *S100a8* expression in the liver and aorta. *n*=3. **p*<0.05, ***p*<0.01, ****p*<0.001.